Semi-solid redox flow battery

by Mihai Duduta

Submitted to the Department of Materials Science and Engineering in partial fulfillment of the requirements for the degree of Bachelor of Science at the

MASSACHUSETTS INSTITUTE OF TECHNOLOGY

June 2010

Signature redacted

Author .....
Department of Materials Science and Engineering
May 11th 2010

Signature redacted

Certified by .....
Yet-Ming Chiang
Professor of Materials Science and Engineering
Thesis Supervisor

Signature redacted

Accepted by .....
Lionel C. Kimerling
Chair, Undergraduate Committee

Semi-solid redox flow battery

by Mihai Duduta

Submitted to the Department of Materials Science and Engineering on May 11th 2010 in partial fulfillment of the requirements for the degree of Bachelor of Science

Abstract:

I have implemented a novel energy storage system, combining the best attributes of the materials used in Li-ion batteries and the design and functioning of a redox flow cell. The use of Li-ion battery materials offers significant increases in energy and power density (200 Wh/kg compared to 25-35 Wh/kg for current commercial vanadium redox batteries). The implementation of a redox flow system allows for energy to be stored outside the cell and for the power and energy of the battery to be decoupled. A proof of concept is achieved by successful cycling of anode and cathode suspensions under intermittent flow conditions. The importance of materials' stability to cell life, energy and power densities is discussed. The high energy densities may enable the use of the proposed system in a variety of application, ranging from grid-level storage to fully electric charge.

Thesis supervisor: Yet-Ming Chiang
Title: Professor of Materials Science and Engineering

Acknowledgements:

I want to thank Prof. Chiang and Prof. Carter for their continued support and guidance throughout this project. I feel privileged to have been a member of the outstanding group of people developing this idea in an atmosphere of intellectual excitement, teamwork and inventiveness. I would like to thank Bryan Ho, Dr. Pimpa Limthongkul, Dr. Vanessa Wood, Victor Brunini, Ian Matts, David Young, Jack Wanderman and Rachel Zucker. I also wish to acknowledge the help and advice I got from the other members of the Chiang and Carter research groups. Mike Tarkanian was a great resource for learning how to design and machine the experimental devices needed. In particular Bryan Ho and I worked closely together for the past two years and it has been a very rewarding and productive collaboration.

Contents

Chapter 1

Introduction

I have co-developed and created a new type of battery design: *a semi-solid flow cell (SSFC)*. This battery improves upon the flow battery concept that decouples power delivery from energy storage.

The improvement is an electrochemical fuel that is composed of two types of solid particles suspended in an electrolytic fluid; this composite is a flowable semi-solid. The first solid-particle type is electrochemically active and the other is an electronically conductive additive. The valuable consequences are very high energy density fuels that can be stored peripherally to - and flowed into - the battery's power train (i.e., current collectors and separator).

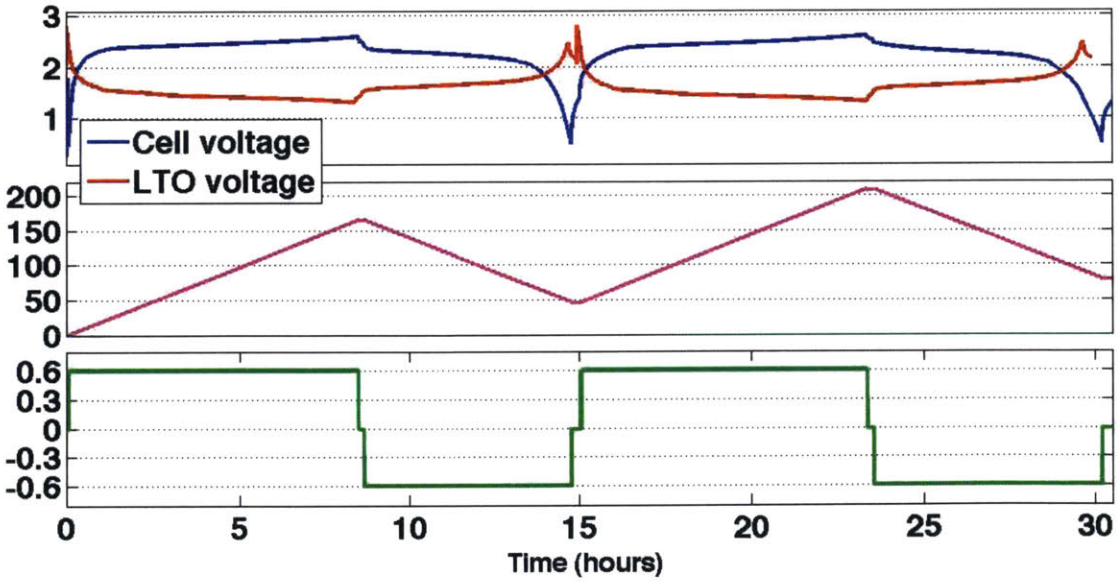

Figure 1.1: Full cell and anode voltages (top: blue, red), capacity (middle: magenta), and current (bottom: green) versus time from a full SSFC (cathode: LCO, anode: LTO, conductive: Ketjen Black additive. This data demonstrates that an SSFC can be charged and recharged. The cell is operated in intermittent mode in which plugs of semi-solids are flowed into the vicinity of the collector and separator, and then flow is stopped while the fuels are charged or discharged. More information regarding this experiment is available in section 5.8.

Two separate semi-solid fuels are required for a full functioning system: 1) anode solid particles co-suspended with conductive particles creating an anolyte that flows into the positive side of the battery during discharge; 2) a catholyte suspension with cathodic and conductive particulates which flow into the negative side of the battery during discharge.

This thesis describes this new invention, the process by which it is realized, and data that characterizes and demonstrates its successful operation. Figure 1.1 illustrates the thesis-denouement: data for voltage-current characteristics of an operating battery with flowing catholyte and anolyte.

The thesis-product, *batteries with flowable semi-solid electrochemical fuels of high energy density*, dramatically lowers cost and increases energy by combining the best attributes of rechargeable batteries and flow cell. They enable economically viable usage-models that can be scaled from transportation and community energy storage to pumped hydroelectric storage for the national power grid.

For example, the SSFC could be used in 200-mile battery electric vehicles (BEVs). To justify this claim, the densities (5.01 g/cm^3 for $LiCoO_2$, 2.2 g/cm^3 for graphite and 1.3 g/cm^3 for typical non-aqeous electrolytes), and specific capacities of the materials used (cathode:140 mAh/g for $LiCoO_2$,; anode: 340 mAh/g for graphite, considering a 2.5 – 3.5 V operating voltage), at 50% volume fraction occupied by solid materials in the suspensions, the energy density would be 278 Wh/kg. The mass of active material needed to power a 50 kW battery electric vehicle would be approximately 180 kg, an acceptable weight by industry standards.

For a grid-storage example, a similar analysis shows that an SSFC-based facility could displace a pumped hydroelectric storage facility (1.9 GW power---15 GWh) at less than 1% of its 842-acre footprint.

Chapter 2

Background: Antecedent Battery Designs

2.1 Rechargeable Li-ion batteries

Commercial Li-ion batteries have been available since the early 1990s, hence the operation of these devices is very well understood. The two main components of the battery the anode and the cathode are electrically connected outside the battery. Common cathode materials are metal oxides, such as $LiCoO_2$, while the most common anode material is graphite. Both of these are mixed with carbon additives (for additional electronic conductivity) and binders. The separator film is usually made of sheets of blended porous polymer, such as polyethylene and polypropylene, which allows the passage of lithium ions while keeping the anode and cathode electrically insulated. The anode, cathode and separator are all soaked in a non-aqueous electrolyte that allows the transport of Li^+ through the battery. Common electrolytes are mixtures of organic solvents (ethylene carbonate, dimethyl carbonate, etc.) and lithium salts ($LiPF_6$, $LiBF_4$, lithium triflate, etc.). All of the above components must be kept dry to prevent dangerous side reactions. In industrial applications this is achievable through the use of dry rooms, while in research and development the use of argon-filled glove boxes is recommended.

Upon charge, an external electrical power source moves electrons from the cathode to the anode. Simultaneously, Li^+ ions are shuttled in the same direction, but through the separator film. During discharge, as Li^+ ions migrate back to the cathode, electrons move through the circuit to accomplish electrical balance. The resulting current allows the battery to function as a remote power source for a number of applications. Figure 2.1 (a) shows a schematic representation of a common lithium ion battery.

Commercialization of Li-ion automotive batteries are primarily driven by their comparatively high specific and volumetric energy densities, approximately 130 Wh/kg and 250 Wh/L. However, in most Li-ion batteries, the volume of active material accounts for less than 50%, the rest being current collectors, separator film, sealing and packaging. The SSFCs that are the subject of this thesis use the high densities of Li-ion battery materials, and reduce the volume fraction of auxiliary material by employing the flow cell strategy described below.

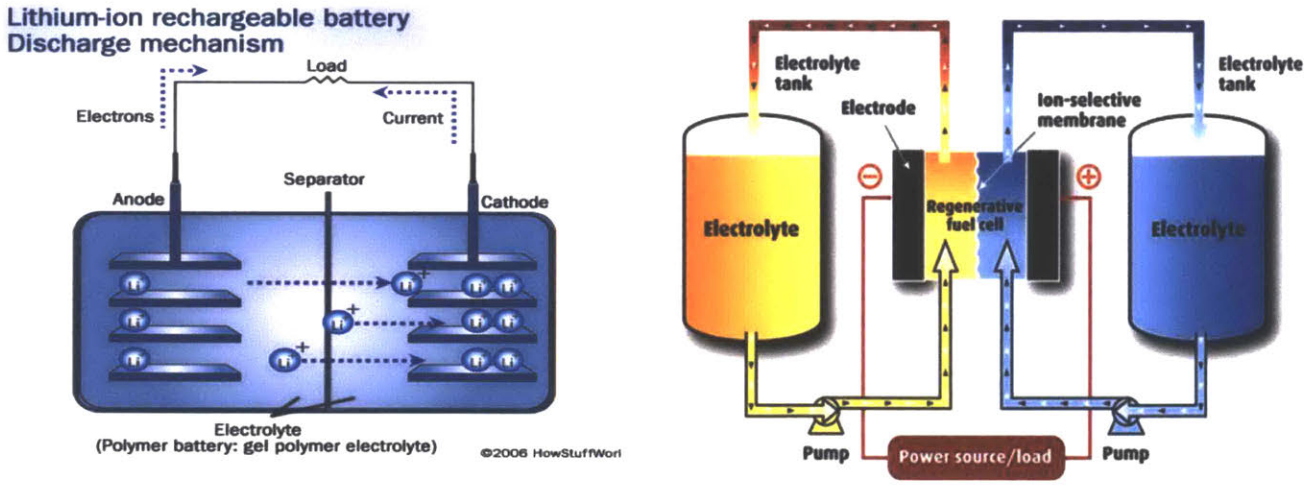

(a) (b)

Figure 2.1 (a) Schematic representation of how a Li-ion battery operates during discharge (Source [1]). (b) Schematic representation of how a redox flow battery operates. (Source [2]).

2.2 Redox flow cells

The operation of a redox flow cell (illustrated in Fig 2.1b) differs from conventional static (e.g., Fig. 2.1a) batteries in that energy capacity is stored in liquids. The catholytic and anolytic liquids are forced to flow from external reservoirs into two channels located between two current collectors and a common ion-selective, non-electronically conducting membrane. The membrane separates the two fluids and must be chemically inert to both the active materials and the components of the electrolyte. Furthermore, it must also have the mechanical strength to withstand the pressure of the solutions while the flow cell is operating. The main advantage of redox flow cells is that power and energy are decoupled: the volume of the storage tank can be increased for larger energy capacity and the collector-membrane-collectors designed and stacked for higher power.

Common redox couples in commercial redox flow batteries include: vanadium redox, $(-)|V^{2+},V^{3+}|V^{4+},V^{5+}|(+)$[3] and polysulfide/bromide, $(-)|S^{0},S^{+}|Br^{-},Br^{0}|(+)$[4] in aqueous electrolytes. For a vanadium redox flow cells, the reactions occurring during charge are described below:

Positive electrode:

$$VO^{2+} + O^{2-} \rightarrow VO_2^{+} + e^{-} \qquad V=0.9 \text{ V vs. } H_2/H^{+} \text{ electrode}$$

Negative electrode:

$$V^{3+} + e^{-} \rightarrow V^{2+} \qquad V=-0.3 \text{ V vs. } H_2/H^{+} \text{ electrode}$$

The reactions are reversed during discharge. The electrochemical reactions occur during collisions of the active material ions to surface of the current collectors (usually made of graphite). The ion-to-collector collision rate is a increasing function of the solution molarity and flow rate; for example,: current density increases with solution flow rate.

Because they employ aqueous ionic-solutions, flow cell operating voltages have a fundamental

upper limit —above 1.4 volts, at which water electrolyzes (i.e., decomposes into hydrogen and oxygen). This relatively low operating voltage, coupled with the solubility limits of the salts that make up the active materials, determines the low energy and power densities. In addition to these limitations, large pumping rates have delayed development and commercialization. Several chemistries based on non-aqueous solvents have been proposed [5], but their stability and solubility are not as high as those of aqueous systems. For comparison: the materials used in commercial vanadium redox batteries retain >50% of their capacity over 1000s of cycles, while materials used in non-aqueous redox batteries lose >90% of their capacity in the first 100 cycles.

Typical current densities for the bromine/polysulfide battery and vanadium redox are in the range of 40 mA/cm^2, with the power densities of approximately 60 mW/cm^2. The specific power densities for vanadium redox are in the 25-35 Wh/kg range, which is considered too low for vehicle applications. [6]

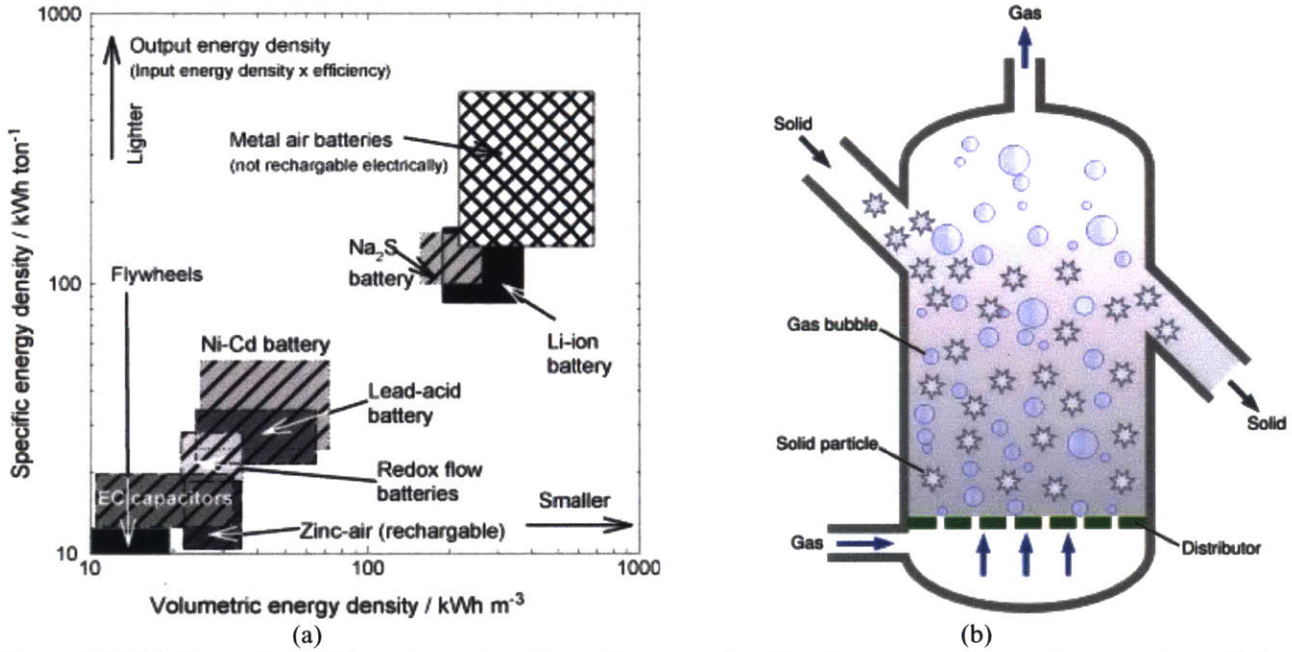

Figure 2.2.1(a) Comparison of the volumetric and specific energy densities for common energy storage systems. Li-ion batteries have approximately 10 fold the volumetric energy of common redox flow cells, which makes them more suitable for vehicle applications.[6] (b) Schematic of the functioning of a fluidized bed reactor. The solid particles can be brought into the reactor, then settled on the distributor. In a battery set up, the distributor would be replaced by a separator film and current collector to allow the electrochemical reaction. The gas can be replaced by pure electrolyte to push the charged (or discharged) solid particles up and out of the reactor. [7]

2.3 Fluidized bed reactors

The operation of a fluidized bed reactor (FBR) is illustrated in figure 2.2.1b. It shares some similarity to flow cell batteries and the SSFCs in this thesis, but has fundamentally different conduction and lithium storage mechanisms. In an FBR, particles are flushed into a reaction chamber with fluid flow; then, as the fluid flow is reduced, the particles settle the bottom. While settled, the particles can react; once the reaction is complete, the particles can be resuspended by increasing the velocity of the flow

through the bottom of the reactor. The depleted particles can be taken out of the reaction chamber while under increased flow, and the reactor can be replenished with fresh material.

The fluidized bed reactor has been used in redox flow batteries, particularly in those which employ zinc, as the reduced form Zn^0, is stable as a solid and needs to be suspended [8]. In fluidized beds, as in typical redox flow cells, electrons are conducted by through particle---particle and particle---current collector collisions. Energy storage occurs via precipitation of material from the solution. In the SSFC system, there is a partial or complete percolation path throughout the suspension because of the carbon additives included; charge storage occurs via ion insertion into solid particles. The percolation network is presumed to increase the current density, and corresponding energy density, by increasing the available contact points between the suspension and the current collector. The necessity of pumping solid material through a reaction chamber suggests that a fluidized bed reactor could be used as a model for the proposed solid suspension redox flow battery.

2.4 Aspects of Li-ion batteries relevant to the semi-solid fuel cells.

The current construction and operation of Li-ion batteries is influenced by a series of factors:

- electrolyte conductivity;
- current collector voltage operating range;
- separator film structure;
- electrolyte stability.

The maximum ionic conductivity of Li ions in commercial electrolytes approaches 0.01 S/cm, as determined by conductivity studies performed in our laboratory. This value is relatively lower than that of aqueous electrolytes: 0.1-0.6 S/cm in common vanadium redox flow cells. [9]

The wide operating voltage range of common Li-ion batteries causes the two current collectors to be made of different metals, which are stable at those respective potentials. For the anode operating in the 0 to 2.5 V vs. Li/Li^+ range, the material of choice is copper. For the cathode, which operates in the 2 to 4.7 V range the material of choice is aluminum. While copper is thermodynamically stable in its operating voltage range, aluminum is kinetically stable due to a passivating oxide layer ,which forms instantaneously on exposure to air. [10] The layer is chemically resistant enough to survive cycling at high rates and high voltages.

Most separator films are designed to be very thin, in the range of 25-50 μm to minimize the polarization across the membrane during charging and discharging of the cell. Due to this requirement, high mechanical strength is not mandatory for application of these film in common Li-ion batteries. However, in the proposed SSFC system, these membranes must be able to withstand pressure from the suspensions being pumped continuously or intermittently on one or both sides. The mechanical resistance of the chosen separator film must be taken into account when planning the operation of the

flow cell.

The pore size of separator film is critical for high performance of the SSFC. The pore size must be large enough to allow lithium ions to pass through, but small enough to prevent the particles which from the suspension from mixing. The current pore sizes of commercial separator films range from 0.02 to 0.05 μm, which corresponds to the desired size. An interesting application would be one in which the electrolyte used for the anode would be different from the one used for the cathode because of stability and solubility concerns. In this case the separator film would have to serve an additional role: to prevent the organic solvent molecules and dissolved ions from passing through and mixing. The pore size needed would be much smaller than that required to prevent passing of particles. Separator films with pore sizes in this range are still being developed and are not yet commercially available.

The stability of most electrolytes is influenced most dramatically by the formation of a solid electrolyte interface (SEI). [11] Typical organic solvents used in Li-ion batteries, such as ethylene carbonate and dimethyl carbonate are not stable at potentials close to that of lithium. The common reaction they undergo is decomposition with the formation of a thin electrically insulating layer on the metal current collector. The formation of a thin and robust SEI allows the other organic solvent molecules to be kinetically stable in the operating potential range. Because the SEI is ionically conductive, it allows the battery to cycle and thus operate properly. However, in the SSFC system, SEI formation can be viewed as a potential problem. If the active material, which is suspended in solution were to be coated with a layer of non-conductive material, this could render it unusable. Because of the complexity of the problem the exact impact of SEI formation must be evaluated during charge and discharge experiments on flowing suspension.

2.5 Anode and cathode material properties

Table 2.1 Presents the voltage at which the materials tested plateau during charging or discharging against a Li/Li^+ electrode, data on density and the specific capacity of the material.

Material	Voltage plateau (V)	Density (g/cm^3)	Specific capacity (mAh/g)
$LiCoO_2$	3.9	5.01	140 [12]
$LiFePO_4$	3.4	3.6	170 [13]
$Li_4Ti_5O_{12}$	1.55	3.46	170 [14]
Graphite	0.1	2.2	340 [15]

Electrochemical reactions:

The electrochemical reactions depend on the whether the material is acting as a cathode or anode in the system. The following electrochemical reactions happen while the system is charging (i.e. storing energy from an external source).

Cathodes:

Lithium cobalt oxide (LCO):

$LiCoO_2 \rightarrow 0.5\ Li^+ + 0.5\ e^- + Li_{0.5}CoO_2$ Reaction potential: 3.9 V vs. Li/Li^+

Lithium iron phosphate (LFP):

$LiFePO_4 \rightarrow Li^+ + e^- + FePO_4$ Reaction potential: 3.4 V vs. Li/Li^+

Anodes:

Lithium titanium oxide (LTO):

$Li_4Ti_5O_{12} + 3\ Li^+ + 3\ e^- \rightarrow Li_7Ti_5O_{12}$ Reaction potential: 1.55 V vs. Li/Li^+

Graphite:

$C_6 + Li^+ + e^- \rightarrow C_6Li$ Reaction potential: 0.1 V vs. Li/Li^+

Chapter 3

Project Description

3.1 Project roadmap

The central goal of this project was a demonstration of the solid suspension redox flow cell. In this novel device, the active materials are suspensions of Li-ion battery anode and cathode materials, mixed with appropriate amounts of carbon additive and electrolyte. These suspensions have to be able to cycle against a Li/Li^+ electrode or another semi solid mixture, under static or flowing conditions. The resulting system is projected to have higher energy densities than typical redox flow cells because of the incorporation of the energy dense materials used in Li-ion batteries. Compared to current automotive batteries, the advantage of the SSFC system consists of the ability to easily replenish the battery with fresh charged material after a full cell discharge, as the active materials are fluids. The theoretical energy density of the system suggests that the SSFC could be a viable solution for automotive applications, enabling fully electric vehicles with fast and safe recharge ability.

This demonstration required that several independent technical hurdles had to be overcome. Those hurdle are illustrated in the roadmap illustrated below.

Key milestone targets:

- preparation of a stable mixture of active material and carbon additive suspended in electrolyte;
- building devices for electrochemical testing of suspensions under static and flowing conditions;
- demonstration of charge/discharge for cathode and anode suspensions under static conditions;
- analysis of cycling performance of suspensions under continuous and intermittent flow conditions;
- investigation of electrolyte on suspension stability and electrochemical performance;
- energy and power density evaluation of the suspensions;
- demonstration of a charging/discharging in a full SSFC cell while remaining stable and suspended.

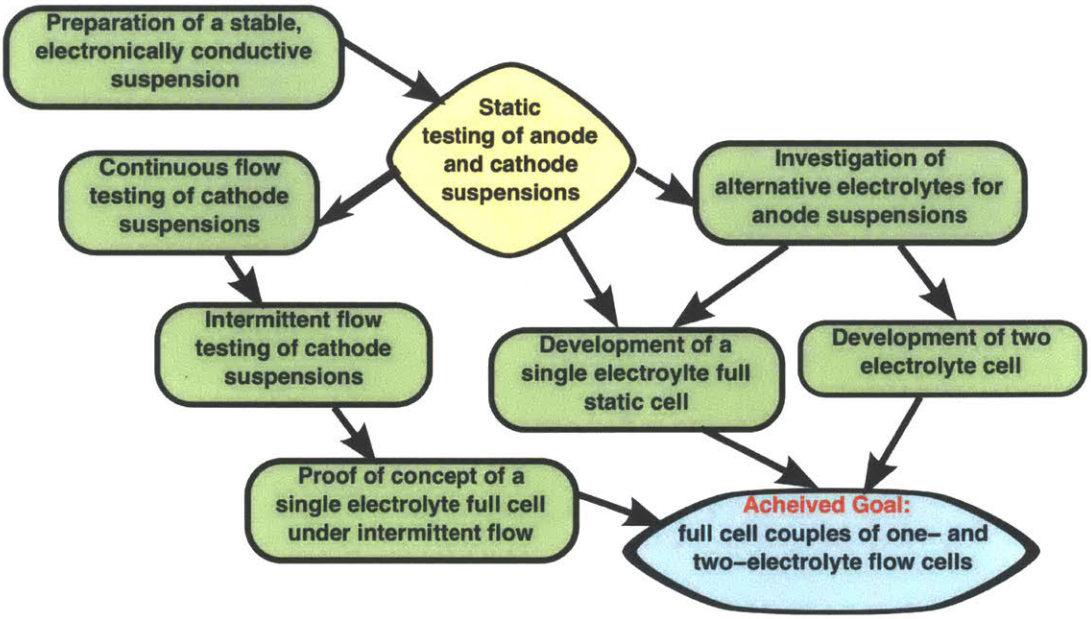

The primary task was the development of a process to co-suspend anode, cathode and carbon-additive particulate materials in electrolytes. These suspensions have to be able to cycle against a Li/Li^+ electrode or another semi solid mixture, under static or flowing conditions.

Towards this end, suspensions of anode and cathode materials were prepared and characterized. The most stable and most conductive materials were electrochemically tested under static conditions. The best performing suspensions of cathode materials were then tested under continuous and intermittent flow conditions. Several different electrolytes were employed in the testing of anode suspensions in order to determine which had the most suitable stability range. The power and energy densities of these systems were evaluated and compared to current high performance flow cell and fuel cell technologies.

To reach the central goal of the project, anode and cathode suspensions were tested against each other under static and intermittent flow conditions in both single and two-electrolyte systems. The success of this experiment served as a proof of concept for the solid suspension flow cell system. Directions for future improvement are proposed, using the best attributes of both the anode and cathode suspensions tested.

3.2 Team roles and responsibilities

The project was developed as a team effort and the contributions of all the team members represented significant progress for the project. The author of this thesis was primarily responsible with electrochemical testing of the suspensions, under static and flowing conditions, and investigation of

electrolyte stability. Graduate student Bryan Ho worked towards developing robust testing cells for static and flow tests as well as understanding the conductivity of suspensions as a function of shear rate; Dr. Pimpa Limthongkul, with the aid of undergraduate students Ian Matts and David Young, worked on alternative chemistries; Dr. Vanessa Wood investigated the microstructure of the suspensions, through TEM imaging, conductivity studies and rheological measurements; undergraduate student Jack Wanderman investigated pumping methods for high viscosity suspensions; graduate student Victor Brunini developed simulation tools for better understanding of flow patterns and conductivity paths for suspensions; Rachel Zucker studied alternative cell designs.

Chapter 4

Experimental methods

4.1 Materials used

The provenance and processing of the materials used is listed based on their role in the functioning of the cell. Appendix 1 contains particle size distribution data for the solid materials listed below.

Cathodes:	-lithium cobalt oxide ($LiCoO_2$) from Seimi, jet milled;
	-Nanophosphate™ olivine from A123 Systems, proprietary composition.
Anodes:	-graphite (MCMB: Meso Carbon Micro Beads), from Osaka Gas Co.
	-lithium titanate ($Li_4Ti_5O_7$), from Altairnano.
Carbon additives:	-Ketjen Black from AkzoNobel.
Electrolytes:	-1,3-dioxolane mixed with LiBETI (lithium bis(pentafluorosulfonyl) imide) (70:30 mixture by mass) (mixture abbreviated as DOL) from Novolyte Inc.
	-alkyl carbonate mixture with $LiPF_6$ (SSDE), from A123 Systems, proprietary composition.
	-1M LiPF6 in dimethyl carbonate (DMC) from Novolyte Inc.
	-2M LiClO4 (99.99% pure, battery grade) in 1,3-dioxolane (99.9% pure, anhydrous) (DXL) prepared from chemicals purchased from Sigma Aldrich.
Separator films:	-Celgard 2500 from Celgard LLC.
	-Tonen from Tonen Chemical Corporation.

All of the materials were dried and stored under argon atmosphere in a glove box to prevent contamination with water or air.

4.2 Suspension preparation:

4.2.1 Suspension sonication:

The active material and carbon (where applicable) were weighed and mixed in a 20 mL glass vial and the solid mixture was suspended by addition of electrolyte. The resulting suspension was mixed and sonicated in a Branson 1510 ultrasonic bath for a period of time ranging from 20 to 60 minutes, depending on the suspension.

4.2.2 Suspension milling:

For powders in which the particles were aggregated, the suspension preparation included a ball-milling step. Milling balls (Yttria Stabilized Zirconia from Advanced Materials, 5 mm in diameter) were added (50 grams for 20 mL of suspension) after the mixing of the powders with the electrolyte. The resulting mixture was sealed from air and humidity and ball milled for 24 hours in a 500 mL zirconia jar at 300 rpms. The resulting suspension was sonicated for 60 minutes.

4.3 Powder processing:

4.3.1 Carbon coating:

The procedure for carbon coating was adapted from a procedure found in literature of coating lithium iron phosphate and was applied to lithium titanium oxide and lithium cobalt oxide.[16] A mixture of pyromellitic acid (from Sigma Aldrich, 96% purity) and ferrocene (from Sigma Aldrich, 96% purity) in a 6:1 ratio by weight was dissolved in acetone with vigorous stirring. The solution was added to the powder to be coated (93 parts by weight, relative to 1 part by weight ferrocene). The suspension was mixed thoroughly and then allowed to dry at 55°C overnight in air. The dried powder was heated under high purity Ar for 10 hours at 800°C in a quartz tube placed inside a Lindberg/Blue M furnace.

4.3.2 Reduction of Lithium Titanate:

The procedure for reduction of lithium titanate ($Li_4Ti_5O_7$ - LTO) was adapted from a similar procedure found in literature.[17] The powder was heated under a gas mixture of Ar and H_2 in a 95:5 ratio at 800°C for 20 hours in a quartz tube placed inside a Lindberg/Blue M furnace. At the end of the reduction, the color of the powder had changed from white to blue.

4.3.3 Copper coating of graphite

The procedure for electroless copper plating of graphite (MCMB) was adapted from a similar procedure found in literature.[18] The graphite particles were cleaned with a 4M solution of nitric acid, then reacted with a 0.1 M $SnCl_2$ solution in 0.1 M HCl for 2 hours. Afterwards the particles were reacted with 0.0058 M $PdCl_2$ in 0.1 M HCl for 2 hours before adding 0.24 M $CuSO_4 \cdot 5\ H_2O$ in a

buffered solution at pH 12 until the solution had changed color from blue to gray. The copper to carbon mass ratio was determined by dissolving the metal on the particles with a solution of 35% nitric acid. The copper content in the resulting solution was determined by Luvak (722 Main St., Boylston MA, 01505) using Direct Current Plasma Emission Spectroscopy conforming to ASTM standard E 1097-07. The Cu:MCMB mass ratio was calculated based on that result.

4.4 Metal part processing:

Gold coating:

In order to reduce the interfacial resistance at the aluminum surface of the parts used in electrochemical testing, the surfaces were coated with gold. The coating was done in a Pelco SC-7 for periods of time from 60 to 300 seconds at 40 mA.

4.5 Electrochemical testing:

4.5.1 Half static cell:

The ability of a suspension to store Li^+ ions against a Li/Li^+ electrode was tested in a static half-cell setup. The experimental setup consisted of a bottom metal piece with a well on top in which the suspension was placed, a piece of separator film (Tonen) covering the well, a slab of lithium metal pressed against a copper cylinder placed on top of the separator film and a hollow copper cylinder

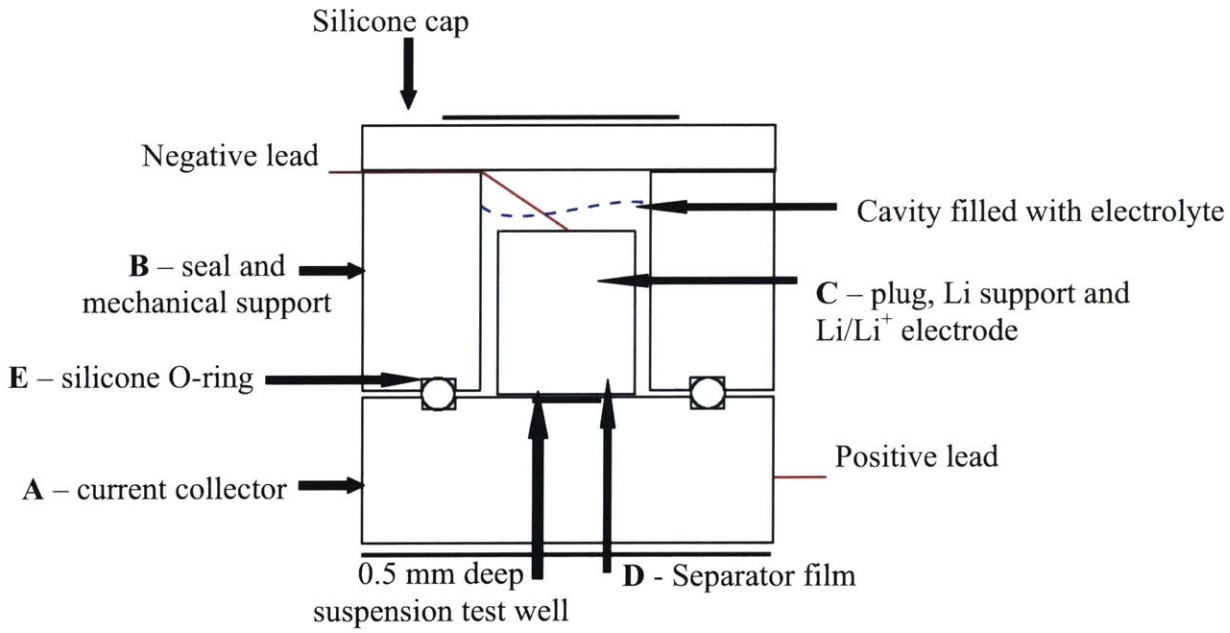

Figure 4.5.1 Schematic of a section through an assembled half static cell. The part labels (**A** – **E**) correspond to the parts in the picture in figure 4.5.2 (a). **A** – 0.5 mm deep testing well for the suspension and current collector, made out of Al for testing cathode suspensions, **B** – sealing support, must be made out of the same material as **C** to prevent corrosion, **C** – Li support and current collector for the Li/Li^+ electrode, **D** – circular separator film (Celgard or Tonen), **E** – Fep-encapsulated silicone O-ring to provide a sufficient seal for the cell and keep **A** and **B** insulated.

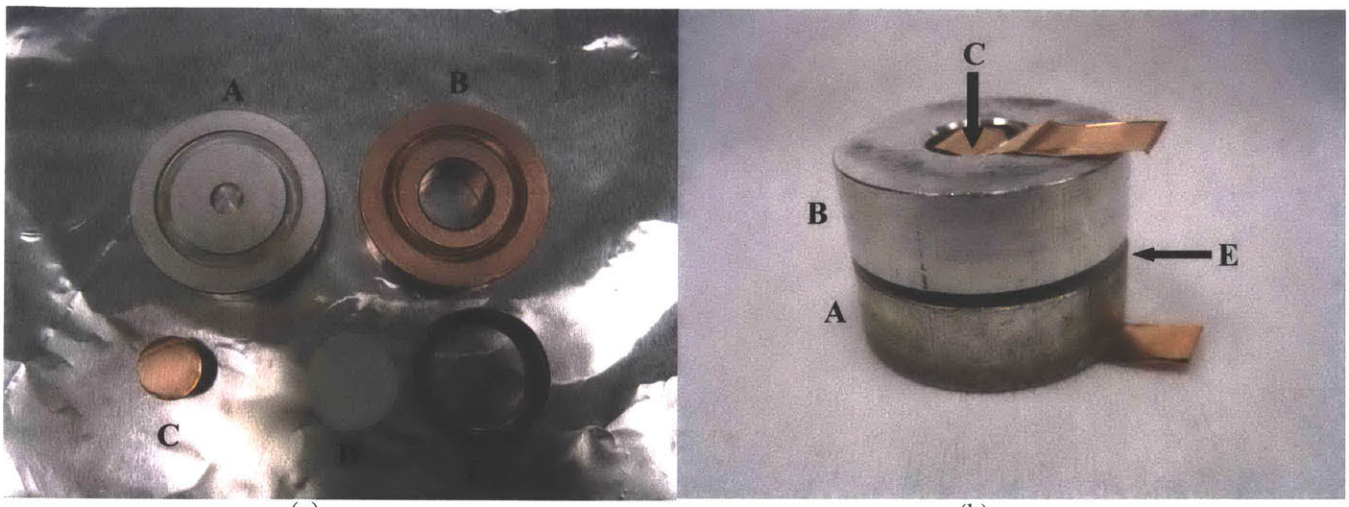

(a) (b)

Figure 4.5.2 (a) Picture of the components of a cathode half static testing cell. **A** – 0.5 mm deep testing well for the suspension and current collector, made out of Al for testing cathode suspensions, **B** – sealing support, must be made out of the same material as **C** to prevent corrosion, **C** – Li support and current collector for the Li/Li^+ electrode, **D** – circular separator film (Celgard or Tonen), **E** – Fep-encapsulated silicone O-ring to provide a sufficient seal for the cell and keep **A** and **B** insulated. (b) Picture of an assembled full cell. The assembling method is identical for half and full cells, the only difference being the material out of which the parts are made of. The components **A** – **E** are stacked to cover the well in A and create a seal to prevent electrolyte evaporation. Copper foil leads are used to connect the cell to the electrodes of the testing instrument. The entire cell is held between the arms of a vice to create a better seal and maintain the parts in place.

surrounding that part. The hollow cylinder and the bottom metal part were insulated through an O-ring made of Fep-encapsulated silicone. The bottom metal part was made of copper alloy 101 for cells operating at potentials in the range 0 to 3 V vs. a Li/Li^+ electrode and of aluminum alloy 6061 for cells operating in the range 1 to 4.5 V vs. a Li/Li^+ electrode. Occasionally, aluminum parts were coated with gold to reduce interfacial resistance via the method described before. The bottom metal part was connected to the positive electrode, while the copper top parts were connected to the negative electrode. The testing was performed using a Solartron Analytical potentiostat operating the 1400 Cell Test System. A schematic of the components of a half static cell is presented in figure 4.5.1, while pictures of the components and assembled cell are presented in figures 4.5.2 (a) and 4.5.3 (a).

4.5.2 Full static cell:

The ability to shuttle Li^+ ions between two different slurries (A and B) was tested in a static full cell setup. The experimental setup consisted of a bottom metal piece with a well on top in which suspension A was placed, a piece of separator film (Tonen) covering the well, a metal cylinder placed on top of the separator film with a well filled with suspension B touching the separator film, and a hollow metal cylinder surrounding that part. The top hollow cylinder and the bottom metal part were insulated through an O-ring made of Fep-encapsulated silicone. The metal parts were made of copper alloy 101 for cells operating at potentials in the range 0 to 3 V vs. a Li/Li^+ electrode and of aluminum alloy 6061 for cells operating in the range 1 to 4.5 V vs. a Li/Li^+ electrode. Occasionally, aluminum parts were coated with gold to reduce interfacial resistance via the method described before. The bottom and top

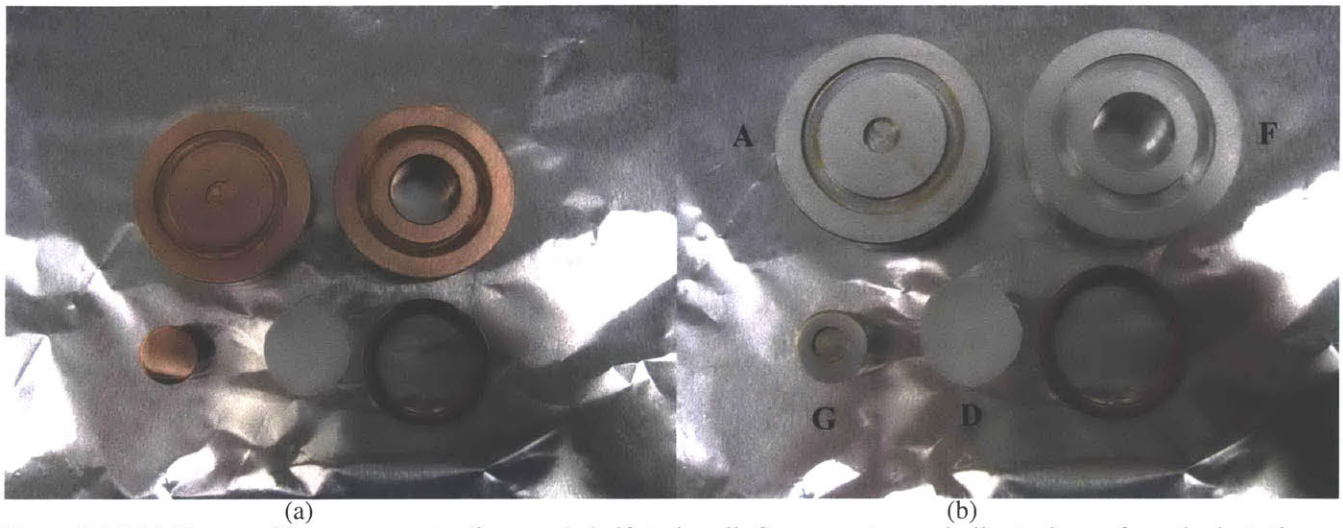

(a) (b)

Figure 4.5.3 (a) Picture of the components of an anode half static cell. Components are similar to those of a cathode testing cell, but the current collector is made out of copper, instead of aluminum, to prevent corrosion reactions. (b) Picture of the components of a full static cell. Main differences from a half cell: **F** – made out of aluminum, same as **G**, to prevent corrosion at the current collector; **G** – plug with a 0.5 mm well, in an assembled cell, the wells in **A** and **G** are facing each other with a separator film in between (**D**). Li^+ ion transport occurs through the separator film during charge and discharge. The parts were made out of aluminum as it showed the lowest interfacial resistance for testing $LiCoO_2$ against $Li_4Ti_5O_7$ in a full cell.

metal parts were connected to the positive and negative electrodes of the potentiostat depending on the respective slurries tested. Figure 4.5.2 (b) shows an assembled full static cell, while figure 4.5.3 (b) shows a picture of the components of the cell used for testing lithium cobalt oxide against lithium titanate. The testing was performed using a Solartron Analytical potentiostat operating the 1400 Cell Test System.

4.5.3 Half flow cell:

The ability of a suspension to store Li^+ ions against a Li/Li^+ electrode while flowing was tested in a flowing half cell setup. The experimental setup consisted of a bottom metal piece with a 1/16" diameter

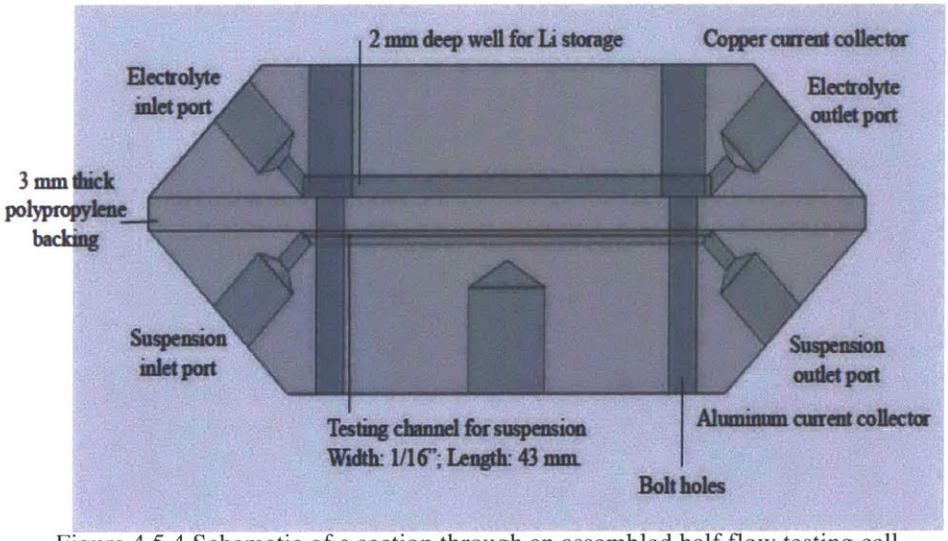

Figure 4.5.4 Schematic of a section through an assembled half flow testing cell.

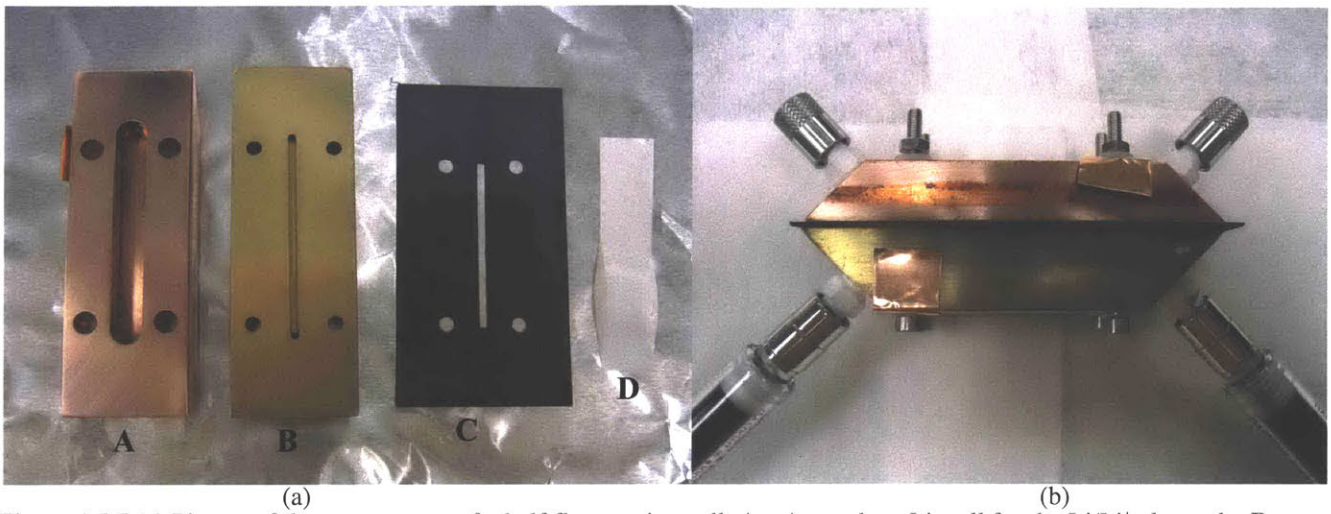

(a) (b)

Figure 4.5.5 (a) Picture of the components of a half flow testing cell. **A** – 4 mm deep Li well for the Li/Li^+ electrode; **B** – testing channel, 1.6 mm wide, 1.4 mm deep, made out of Al, coated with Au for 300 s; **C** – polypropylene spacer (0.017" thick) for mechanical support; **D** – 14 mm x 60 mm separator film (Tonen). (b) Picture of an assembled half flow cell for use in an intermittent flow test. The components are held together using stainless steel nuts and bolts. The Li/Li^+ electrode side is filled with electrolyte and capped off. The active material is loaded and pushed through the testing channel via syringe. Copper foil leads are used to connect the cell to the electrodes of the testing instrument.

channel on top, through which the suspension was flowing, a piece of separator film (Tonen) covering the channel, a piece of polypropylene with a hollowing of the same profile as the channel and a copper piece with a deep well filled with lithium metal. The parts were held together with 316 stainless steel nuts and bolts; shorting the cell was avoided with plastic washers. The two ends of the suspension-filled channel were connected on either side to a piece of Chem-Sure (from Gore™) with 2 pieces of Chem-Durance (from Masterflex) (1/16 inch inside diameter for all pieces of tubing). The Chem-Sure tubing was placed inside a Masterflex US peristaltic pump, which pumped the suspension at rates

(b)

(a)

Figure 4.5.6 (a) Picture of an assembled half flow cell for use in a continuous flow test. The channel is connected via two 4 inch pieces of Chem-Durance tubing (1/16" inner diameter) to a 6 inch piece of Chem-Sure tubing (1/16" inner diameter) to be inserted in a peristaltic pump. The Chem-Sure was used inside the pump because of its higher mechanical strength and chemical stability. (b) Picture of an assembled half flow cell for use in a continuous flow test, inserted into the Masterflex peristaltic pump.

ranging from 0.1 to 15 mL/min. Compared to the Chem-Durance the Chem-Sure was found to maintain elastic properties for longer periods of use in the peristaltic pump. The bottom metal part was made of copper alloy 101 for cells operating at potentials in the range 0 to 3 V vs. a Li/Li^+ electrode and of aluminum alloy 6061 for cells operating in the range 1 to 4.5 V vs. a Li/Li^+ electrode.

Occasionally, aluminum parts were coated with gold to reduce interfacial resistance via the method described before. Where possible, a reference electrode was inserted by replacing the separator film with two pieces of separator film containing a small amount of lithium metal pressed on a thin piece of copper foil. The bottom metal part was connected to the positive electrode, while the copper top parts were connected to the negative electrode. Figure 4.5.4 shows a schematic of an assembled half flow cell, while figure 4.5.5 (a) shows a picture of the components of a half flow cell and figure 4.5.5 (b) shows a picture of a cell used in an intermittent flow test. Figure 4.5.6 (a) shows an assembled half flow cell prepared to be tested in a continuous flow setup, while figure 4.5.6 (b) shows the test cell in the Masterflex pump. The testing was performed using a Solartron Analytical potentiostat operating the 1400 Cell Test System.

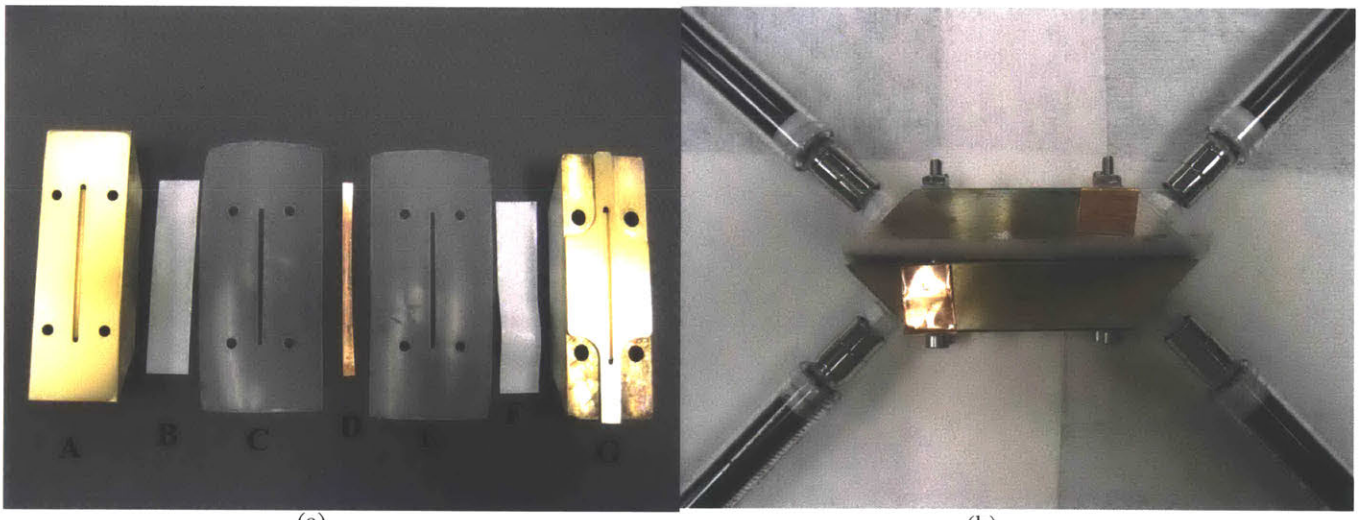

(a) (b)

Figure 4.5.5 (a) Picture of the components of a full flow cell. The cell design is symmetric around **D**, the reference electrode made out of 3 mm x 60 mm piece of copper foil. Li metal was pressed against the copper and the electrode was inserted perpendicular to the channel in the assembled cell. Parts **A** and **G** are testing channels, 1.6 mm wide, 1.4 mm deep, made out of Al, coated with Au for 300 s; parts **B** and **F** are separator films (Tonen, 14 mm x 60 mm); parts **C** and **E** are polyethylene spacers (0.005" thick) for mechanical support. (b) Picture of an assembled full flow cell for use in an intermittent flow test. The components are held together using stainless steel nuts and bolts. The active materials are loaded and pushed through the testing channels on each side via syringe. Copper foil leads are used to connect the cell to the electrodes of the testing instrument.

4.5.4 Full flow cell:

The ability to shuttle Li^+ ions between two slurries (A and B) while flowing was tested in a flowing full cell setup. The experimental setup consisted of two metal pieces with a 1/16 inch diameter channel on top through which the slurries (A and B) were flowing, one or several pieces of separator film (Tonen) covering the entire surface of the pieces. The parts were held together with 316 stainless steel nuts and

bolts; shorting the cell was avoided with plastic washers and with careful polishing of the surfaces of the metal parts. The two ends of the suspension-filled channels were connected on either side for each to a piece of Chem-Sure (from Gore™) with 2 pieces of Chem-Durance tubing (1/16 inch inside diameter for all pieces of tubing). The Chem-Sure tubing sections were placed inside a Masterflex US peristaltic pump which pumped the suspension at rates ranging from 0.1 to 15 mL/min. Compared to the Chem-Durance tubing the Chem-Sure tubing was found to maintain elastic properties for longer periods of use in the peristaltic pump. The bottom metal part was made of copper alloy 101 for cells operating at potentials in the range 0 to 3 V vs. a Li/Li^+ electrode and of aluminum alloy 6061 for cells operating in the range 1 to 4.5 V vs. a Li/Li^+ electrode. Occasionally, aluminum parts were coated with gold to reduce interfacial resistance via the method described before. Where possible, a reference electrode was inserted by replacing the separator film with two pieces of separator film containing a small amount of lithium metal pressed on a thin piece of copper foil. The metal parts were connected to the positive and negative electrodes of the potentiostat depending on the respective slurries tested. Figure 4.5.5 (a) shows a picture of the components of the full flow cell, while figure 4.5.5 (b) shows a picture of an assembled full flow cell for an intermittent flow test. The testing was performed using a Solartron Analytical potentiostat operating the 1400 Cell Test System.

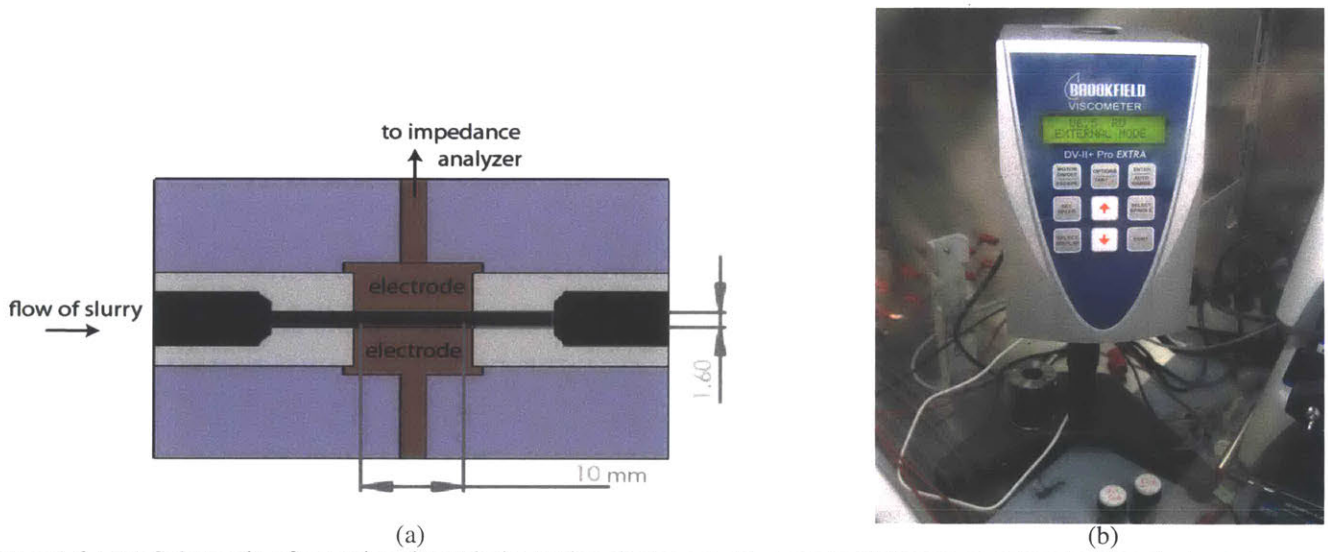

(a) (b)

Figure 4.6.1 (a) Schematic of a section through the testing device used for conductivity measurements. The electrodes were made out of stainless steel, while the rest of the device was constructed out of PVDF for chemical and mechanical stability. (b) Picture of the digital viscometer used in rheological measurements inside the Ar-filled glove box.

4.6 Conductivity measurements

The conductivity of solid suspensions in electrolyte was measured in both static and flowing conditions in a parallel plate setup. The measuring device was constructed in lab using stainless steel plates (3 mm x 10 mm; 1.6 mm spacing in between the plates) and was connected to the FRA Analyzer of the 1400

Cell Test System. Conductivity was determined by varying the frequency of an AC current from 0.1 to 10^6 Hz and analysis of the resulting Nyquist plot of imaginary vs. real parts of the resistance. Figure 4.6.1 (a) shows a schematic of the test cell used in the conductivity measurements.

4.7 Rheological measurements

The viscosities of particle suspensions in electrolyte was measured inside the glove box using a Brookfield Digital Viscometer, mode DV-II+ Pro Extra. The measurements were conducted as quickly as possible to minimize the degree of solvent evaporation from the suspension and modification of rheological properties. The experimental setup consisted of varying the shear rate between 5 and 35 sec^{-1} in increments of 5 sec^{-1}. A each shear rate, 30 data points for viscosity are taken over the course of a minute. The resulting data is plotted correlating viscosity to the shear rate applied. Figure 4.6.1 (b) shows a picture of the digital viscometer used in the measurements inside the glove box to prevent suspension exposure to oxygen and moisture.

Chapter 5

Results and Discussion

5.1 Preparation of a stable, conductive suspension

Initial tests showed that the active materials formed stable suspensions only for a limited time and only at high loading volume fractions (45% for LCO, 30% LTO, 35% MCMB). However, when tested in a static cell setup, these suspensions showed very high polarization when charged at relatively low rates (C/20). The low current was assumed to be due to the low conductivity of the suspensions. The addition of conductive carbons (Ketjen Black) had two desired effects: an increase in the electronic conductivity of and stabilization of the suspensions. The direct effect of increase in electronic conductivity was the ability of suspensions to be cycled consistently within a wide range of currents (2.5C – C/20) depending on the ratio of active material to carbon additive. Figure 5.1.1 shows a qualitative picture of the relative stability of slurries with and without carbon additives.

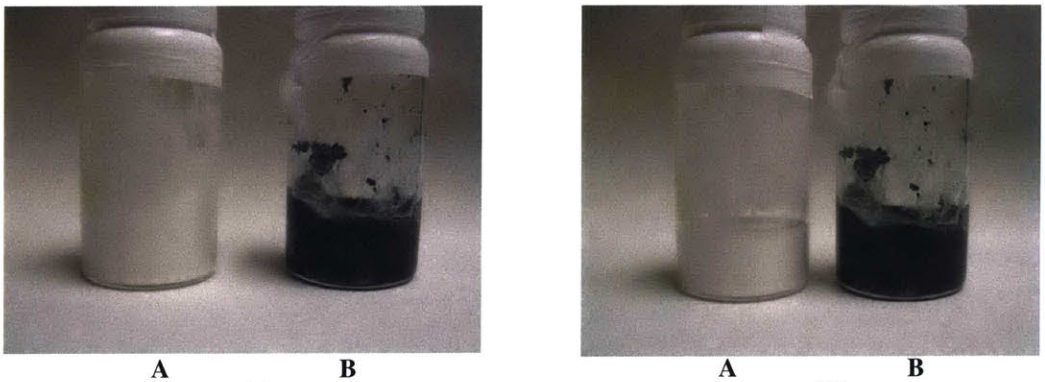

(a) (b)

Figure 5.1.1 Pictures of suspensions of lithium titanate (LTO) in organic electrolyte **A** without carbon additive and **B** with carbon additive. (a) Picture taken after sonication for 60 minutes. (b) Picture taken of sonicated suspensions after 24 hours. The carbon-less suspension is settled towards the bottom of the vial and has a clear electrolyte supernatant on top. The suspension which contains carbon is still suspended and the LTO has not settled at the bottom.

The rheological properties of suspensions of active material (Lithium Cobalt Oxide – $LiCoO_2$ – LCO) mixed with carbon additive (Ketjen Black) were analyzed. Figures 5.1.2 presents viscosity vs. shear rate data for suspension containing just LCO, just Ketjen Black and mixtures of the two in

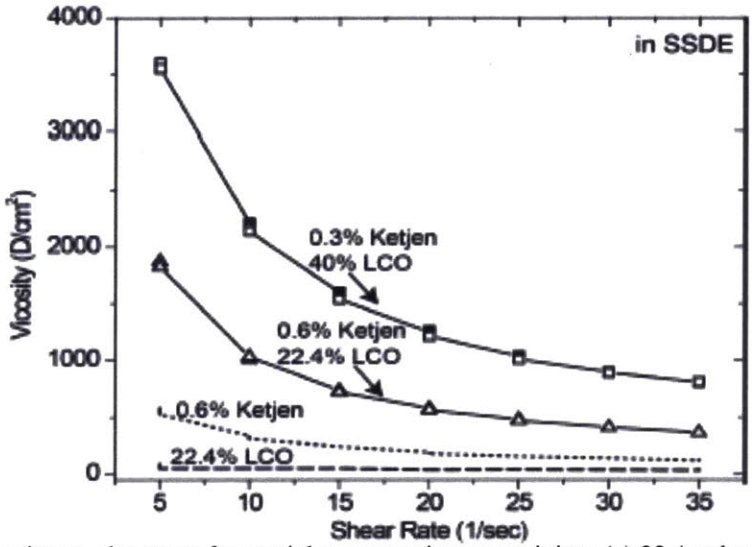

Figure 5.1.2 Plot of viscosity vs. shear rate for particles suspensions containing: (a) 22.4 volume % LCO in SSDE, (b) 0.6% Ketjen in SSDE, (c) 22.4% LCO and 0.6% Ketjen in SSDE and (d) 40% LCO and 0.3% Ketjen in SSDE. The shear rate is varied between 5 and 35 sec^{-1} in increments of 5 sec^{-1}. A each shear rate, 30 data points are taken over the course of a minute. All suspensions show shear thinning behavior. Carbon black and LCO suspended in SSDE have extremely low viscosities (see dotted and dashed lines), but combining these two systems significantly increases their net viscosity. This is attributed to the formation of LCO particulate networks, with LCO particles linked by the Ketjen. Data courtesy of Dr. Vanessa Wood.

different ratios. The data suggests that mixing the two solid components creates particulate networks, in which LCO particles are connected by Ketjen aggregates. This results is consistent with qualitative observations which correlated the suspension stability with increased carbon content and increased viscosity. Subsequent tests of mixtures with other active materials (lithium titanate, graphite) and other electrolyte systems (DOL) showed similar trends of viscosity vs. shear rate. The viscosity data was collected by Dr. V. Wood.

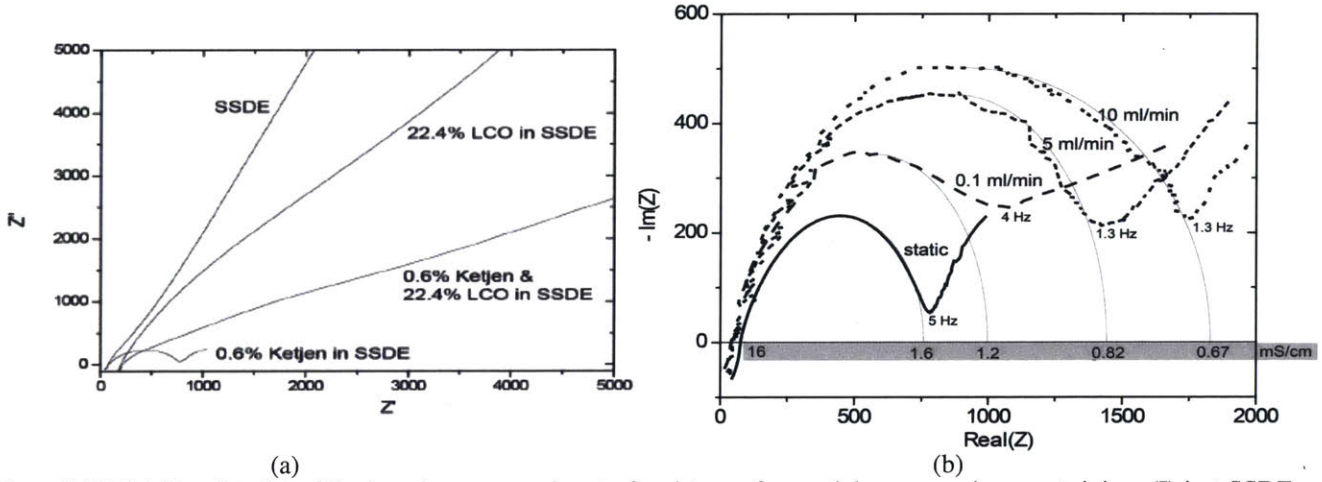

(a) (b)

Figure 5.1.3 (a) Nyquist plot of the imaginary vs. real part of resistance for particles suspensions containing: (I) just SSDE, (II) 22.4 volume % LCO in SSDE, (III) 22.4% LCO and 0.6% Ketjen in SSDE and (IV) 0.6% Ketjen in SSDE under static (non-flowing) conditions. The conductivity of the materials is dominated by the conductivity of the electrolyte. In mixed Ketjen and LCO suspension, electrical conductivity is dominated by the LCO particles. (b) Nyquist plot for 0.6% Ketjen in SSDE under different flow conditions. The changes in shape of the curves at different flow rates shows that flow has an effect on the microstructure of the Ketjen aggregates. The highlighted numbers in the lower portion of the figure correspond to the estimated electronic conductivity of the suspensions in mS/cm. Data courtesy of Dr. Vanessa Wood.

The electronic conductivities of lithium cobalt oxide (LCO) and Ketjen suspensions were determined under both static and flowing conditions. Figure 5.1.3(a) presents Nyquist plots correlating the imaginary vs. real parts of the resistance of the suspensions in AC testing conditions. Under static conditions, the conductivity of the electrolyte appears to dominate the overall conductivity of the suspensions, except for those containing only carbon additive. That specific suspension was also tested under flow conditions with increasing flow velocity. The results, presented in figure 5.1.3(b) showed that as the flow rate was increased, the electronic conductivity of the suspension decreased most likely because the available percolation paths were disrupted. Data collected by Dr. V. Wood.

5.2 Charge/discharge experiments on stable cathode suspensions

The ability of stable suspensions to shuttle lithium ions while under zero flow was tested in a static cell setup described in section 3.5.1. In this type of experiment, the suspension filled a well which was covered with a separator film, then capped by a Li/Li^+ electrode. The assumption behind the test was that a percolating network is formed in the suspension through which all of the active material in the cell is connected to the current collector. Figure 5.2.1 shows the voltage and charge profiles of two different cathode materials which exhibit excellent cycling behavior.

Figure 5.2.1(a) represents the first ever successful cycling of a suspension of lithium cobalt oxide ($LiCoO_2$ – LCO, as received) mixed with Ketjen Black in organic carbonate electrolyte (SSDE) (Experiment Static-Cathode-1). The graph displays voltage as a function of the capacity of the material, a common performance metric for Li-ion battery materials. The flat plateaus on both charge and discharge suggests that the electrochemical reaction is highly reversible, while the operating voltage is close to 3.9 V vs. Li/Li^+, the expected value for an lithium cobalt oxide (LCO) cathode. The hysteresis of the charge and discharge voltage curves is small, which translates into a high energy efficiency. The charge rate of the cell is C/20, meaning that at the current running through the cell, the material will be fully charged in 20 hours. A discharge of D/20 represents the rate at which the cell fully discharges in 20 hours. Overall, this represents an excellent result, showing for the first time ever, the ability of a cathode mixture to charge and discharge, while remaining suspended.

Comparatively, figure 5.2.1(b) represents the cycling behavior of a different lithium cobalt oxide mixture at significantly higher rates (Experiment Static-Cathode-2). The main difference in suspension composition is due to jet milling of the lithium cobalt oxide (LCO) powder, which allowed more active material to be suspended. Also, less carbon additive was needed for the suspension to be able to cycle in a static cell setup. The rate at which this cell can be operated is C/3.2 and D/3.2, which suggests that these materials are suitable for high power applications with short discharge times. There is significantly more hysteresis in the charge vs. discharge voltage curves as the polarization (a sum of the internal resistances in the cell) is increased because of operation at higher currents. The reversible capacity is also decreased from the theoretical limit of 140 mAh/g LCO to 105 mAh/g LCO. At these rates, both the lower energy efficiency and lower reversible capacity are expected, as they are common

for all Li-ion battery materials. However, the discharge voltage is still high (>3.5 V for 80% of the reversible capacity), and the voltage plateaus are still considerably flat, which supports the use of these materials in high power applications.

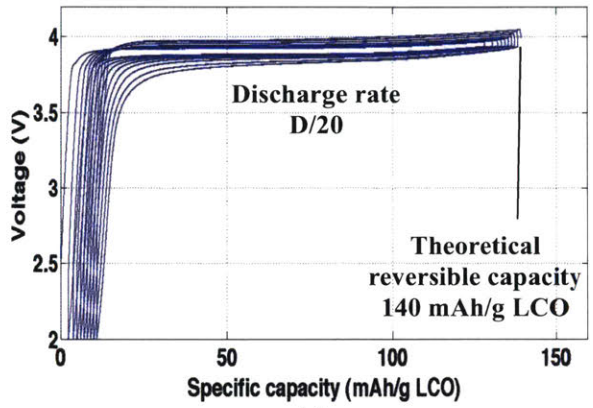

(a)

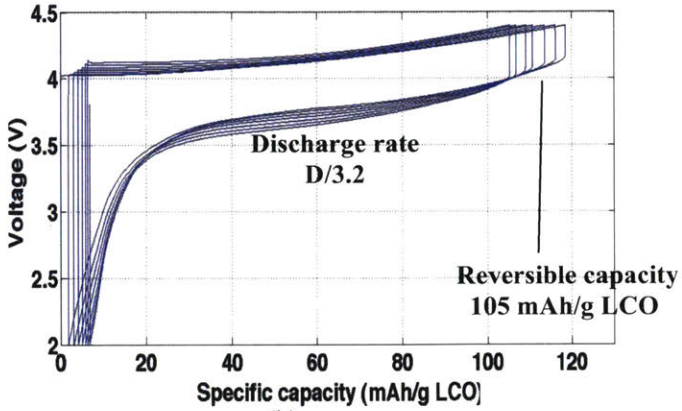

(b)

Figure 5.2.1 (a) Voltage vs. specific capacity profile for a cathode suspension tested in a half static cell setup (experiment Static-Cathode-1). The data shows a suspension of LCO and carbon additive can cycle Li^+ ions against a Li/Li^+ electrode at C/20 rates (specific current = 7.0 mA g^{-1} LCO, current density = 1.3 A m^{-2} Celgard). (b) Voltage vs. specific capacity profile for a cathode suspension tested in a half static cell setup (experiment Static-Cathode-2). The data shows the ability of a suspension of LCO and carbon additive to cycle at C/3.2 rates (specific current = 44.1 mA g^{-1} LCO, current density = 31.2 A m^{-2} Celgard).

Table 5.2.1 Description of experimental setup of test Static-Cathode-1. LCO was used as received.

Test type: half static cell		Current collector: Aluminum		Separator film: Celgard	
Suspension composition:		Coating: N/A		Test cell characteristics:	
Volumetric	By mass:	Suspension characteristics:		Well depth	0.3 mm
12.0 % LCO	35.1 % LCO	Theoretical energy density:		Cell volume	9.5 µL
1.5 % Ketjen	1.8 % Ketjen	Volumetric	84.2 mAh/mL	Theoretical capacity	0.80 mAh
86.5 % SSDE	63.1 % SSDE	Gravimetric	45.4 mAh/g	C rate @ 40 µA	C/20

Table 5.2.2 Description of experimental setup of test Static-Cathode-2. LCO used was jet milled.

Test type: half static cell		Current collector: Aluminum		Separator film: Celgard	
Suspension composition:		Coating: N/A		Test cell characteristics:	
Volumetric	By mass:	Suspension characteristics		Well depth	0.55 mm
26.0 % LCO	56.1 % LCO	Theoretical energy density:		Cell volume	17.4 µL
0.8 % Ketjen	0.7 % Ketjen	Volumetric	182.4 mAh/mL	Theoretical capacity	3.17 mAh
73.2 % SSDE	43.2 % SSDE	Gravimetric	78.6 mAh/g	C rate @ 1000 µA	C/3.2

The main target of static cell experiments was to determine how well the cathode materials cycle while being suspended in a carbon and electrolyte mixture. However, figure 3.5.1 shows that the active material is tested in a shallow well covered by separator film and capped by a Li slab as the Li electrode. Because of the design of the cell, the active material could potentially settle at the bottom of the test well. The resulting settled suspension would not have been considered viable for a flow system in which the "fuel" must be pumped in or out of the cell regularly. Also, a settled "cake" of active material could have been cycled without the need of a percolating network throughout the suspension.

For these reasons, a modified half cell static test was done in which the test well had been inverted and was facing downwards. In the modified setup, settling of the active material in the suspension would have determined disconnection from the current collector above. The viscosity of the suspensions was found to increase with an increase in the content of carbon additives. Therefore a suspension with a higher loading of carbon was prepared and tested to avoid leakage out of the test well.

Figure 5.2.2 shows the voltage, charge and current profiles vs. time for a suspension with the composition 40% lithium cobalt oxide (LCO) and 1.5% Ketjen in the inverted static cell setup (experiment Static-Cathode-3). The top plot represents the voltage of the cell against a Li/Li^+ electrode, as a function of time. The operating voltage of the cell is in the 3.7 – 4.2 V, as expected for a lithium

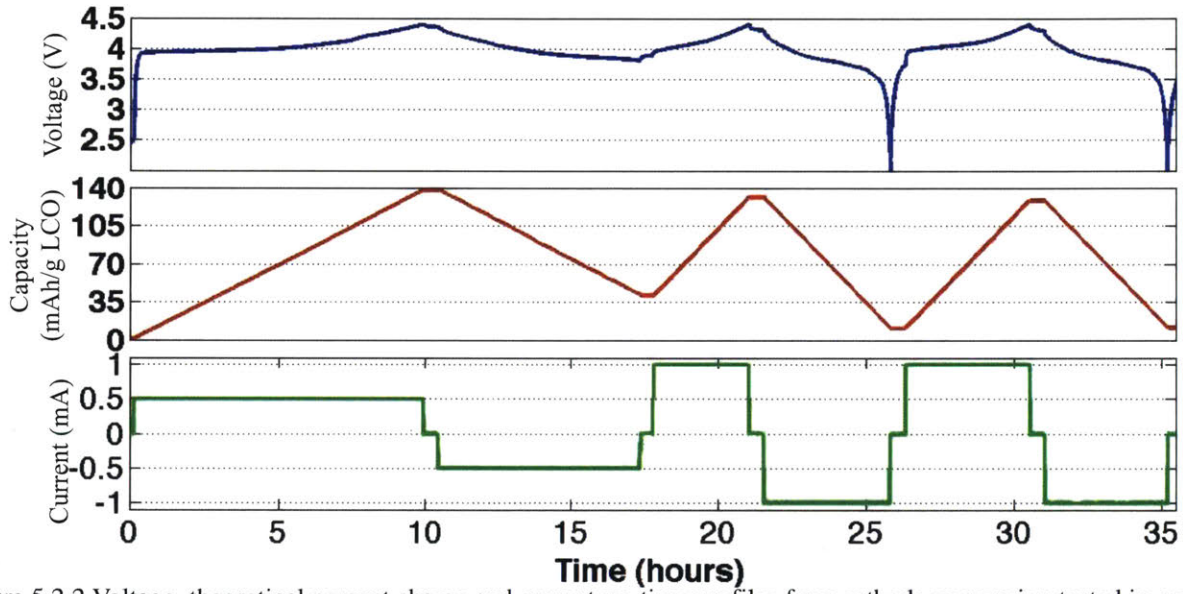

Figure 5.2.2 Voltage, theoretical percent charge and current vs. time profiles for a cathode suspension tested in an inverted half static cell setup (experiment 2C). The data shows the ability of an suspension of LCO and carbon additive to cycle at C/5 rates (specific current = 27.6 mA g^{-1} LCO, current density = 31.2 A m^{-2} Celgard).

Table 5.2.3. Description of experimental setup Static-Cathode-3.

Test type: half static cell		Current collector: Aluminum		Separator film: Celgard	
Suspension composition:		Coating: Au sputtered (120 s @ 40 mA)		Test cell characteristics:	
Volumetric	By mass:	Suspension characteristics		Well depth	0.62 mm
36.0 % LCO	67.0 % LCO	Theoretical energy density:		Cell volume	20.1 µL
1.5 % Ketjen	1.2 % Ketjen	Volumetric	252.5 Ah/L	Theoretical capacity	5.07 mAh
62.5 % SSDE	31.8 % SSDE	Gravimetric	93.4 Ah/kg	C rate @ 1000 µA	C/5

cobalt oxide cell. The middle plot represents the capacity of the material in the cell, per gram of active material (LCO) used. The cell manages to charge to almost full theoretical capacity (140 mAh/g LCO), and has an excellent reversible discharge capacity (120 mAh/g LCO). The bottom plot represents the current running through the cell as a function of time. The graph shows that the cell can charge to more

than 80% capacity at both C/10 and C/5 rates. In this experiment, the time component of the data is very significant, as it shows that over several tens of hours, the suspension is still stable, in spite of the inverted cell setup. For this reason, the voltage, specific capacity and current were plotted as functions of time on the same time axis. This result confirms that the active material does not settle out, but remains suspended, which is one of the main requirements for a solid suspension redox flow cell.

5.3 Importance of electrolyte stability on anode suspension cycling

Static tests of anode materials revealed the importance of SEI formation on the stability of suspensions and their potential use in solid suspension flow cells. Carbonate solvents are known to form a stable solid electrolyte interface, which is non-electrically conductive. For the proposed SSFC system, the coating of suspended particles with a non-conductive layer was considered to be most detrimental as they could no longer charge or discharge in contact with the current collector.

Therefore, a non-carbonate electrolyte was used in the testing of anode materials in suspension. The electrolyte of choice was a mixture of 1,3-dioxolane and LiBETI salt in a 70:30 mass ratio (DOL). Compared to carbonate electrolytes which begin forming an SEI at ~1.5 V, DOL mixed with LiBETI is chemically stable down to ~1.0V, which made lithium titanate ($Li_4Ti_5O_{12}$ - LTO)(lithiation potential = 1.55 V vs. Li/Li^+) the material of choice for anode tests. The low

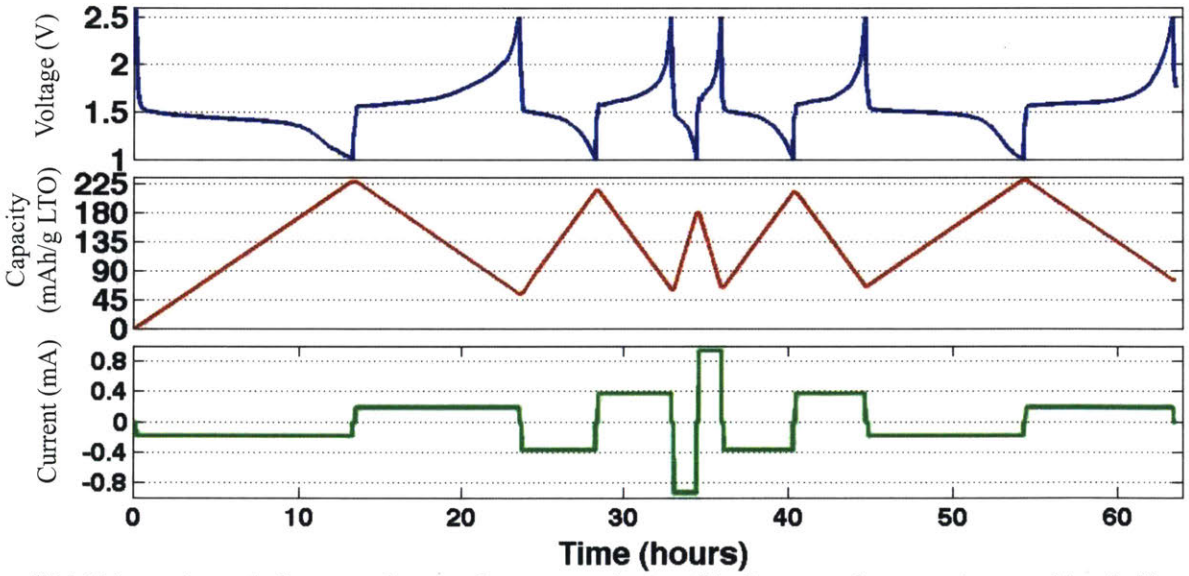

Figure 5.3.1 Voltage, theoretical percent charge and current vs. time profiles for an anode suspension tested in a half static cell setup (experiment 3A). The data shows the ability of an suspension of reduced LTO and carbon additive to cycle in dioxolane based (DOL) electrolyte at C/1.8 rates (specific current = 91.5 mA g^{-1} reduced LTO, current density = 31.2 A m^{-2} Tonen).

conductivity of bulk lithium titanate ($\sigma = 1.0 \times 10^{-13}$ S cm^{-1}) was assumed to be detrimental to the ability of the anode suspension to cycle at high rates. Hence, several processing techniques were used in an attempt to increase electronic conductivity. The most successful method to increase conductivity was reduction under a H_2/Ar atmosphere at 800°C [17]. The metric for conductivity increase was taken

to be reduction of polarization on the suspension during charging and discharging in a static test cell.

The results of a cycling experiment on a suspension prepared with reduced lithium titanate. powder are presented in figure 5.3.1 (experiment Static-Anode-1). The data is presented in the voltage, capacity and current vs. time format. The voltage curve shows plateaus around the voltage of partially charged lithium titanate, at 1.55 V, suggesting that the active material is actually being lithiated and delithiated. The capacity curve shows that the charge capacity exceeds the maximum theoretical capacity of lithium titanate (170 mAh/g), which can be explained by undesired decomposition reactions of the electrolyte during charge. However, the material shows significant (~120 mAh/g LTO) reversible capacity even at high rates (C/1.8 and D/1.8). The current profile shows repeated charge and discharge steps at the following rates: C/9, D/9, C/4.5, D/4.5, C/1.8, D/1.8, C/5, D/5, C/9, D/9. The scope of this type of charge / discharge experimental schedule is to determine the reversible capacity of the material at high rates, and how much of that capacity is still available when the material is cycled again at low rates. The data confirms lithium titanate as a promising anode material in a dioxolane-based electrolyte. Moreover, the reduction of the material makes allows the suspension to be cycled at high rates while retaining significant reversible capacity. This data represents the first successful cycling of a lithium titanate mixture with carbon additive and dioxolane electrolyte (DOL), while remaining a stable suspension.

Table 5.3.1. Description of experimental setup Static-Anode-1, the active material used was reduced Altairnano LTO.

Test type: half static cell		Current collector: Aluminum		Separator film: Tonen	
Suspension composition:		Coating: Au sputtered (300 s @ 40 mA)		Test cell characteristics:	
Volumetric	By mass:	Suspension characteristics		Well depth	0.5 mm
20.0 % LCO red	38.6 % LTO red	Theoretical energy density:		Cell volume	15.8 µL
0.6 % Ketjen	0.7 % Ketjen	Volumetric	117.6 Ah/L	Theoretical capacity	1.83 mAh
79.4 % DOL	60.7 % DOL	Gravimetric	65.7 Ah/kg	C rate @ 1000 µA	C/1.8

The carbonate solvents used in common electrolytes have slightly different stabilities with respect to SEI formation. Acyclic molecules, such as dimethyl carbonate and ethyl methyl carbonate, have been found to be more stable than cyclic one, such as ethylene and propylene carbonate.[19] A more stable electrolyte was prepared by using only 1M $LiPF_6$ in dimethyl carbonate (DMC). A combination of DMC as the electrolyte in the suspension and more conservative voltage cutoff limits for the charge / discharge experiment allowed a lithium titanate (LTO) suspension to cycle statically in a carbonate solvent.

Figure 5.3.2 shows the voltage, capacity and current vs. time profiles for a suspension of Altairnano lithium titanate in dimethyl carbonate electrolyte (concentration: 1M LiPF6, abbreviated as DMC) (experiment Static-Anode-2). The voltage profile shows that the polarization during charge and discharge is very low (>0.1 V), which is most likely due to the shallow testing well as well as the high carbon content of the suspension. The maximum capacity reached during charge is less than the

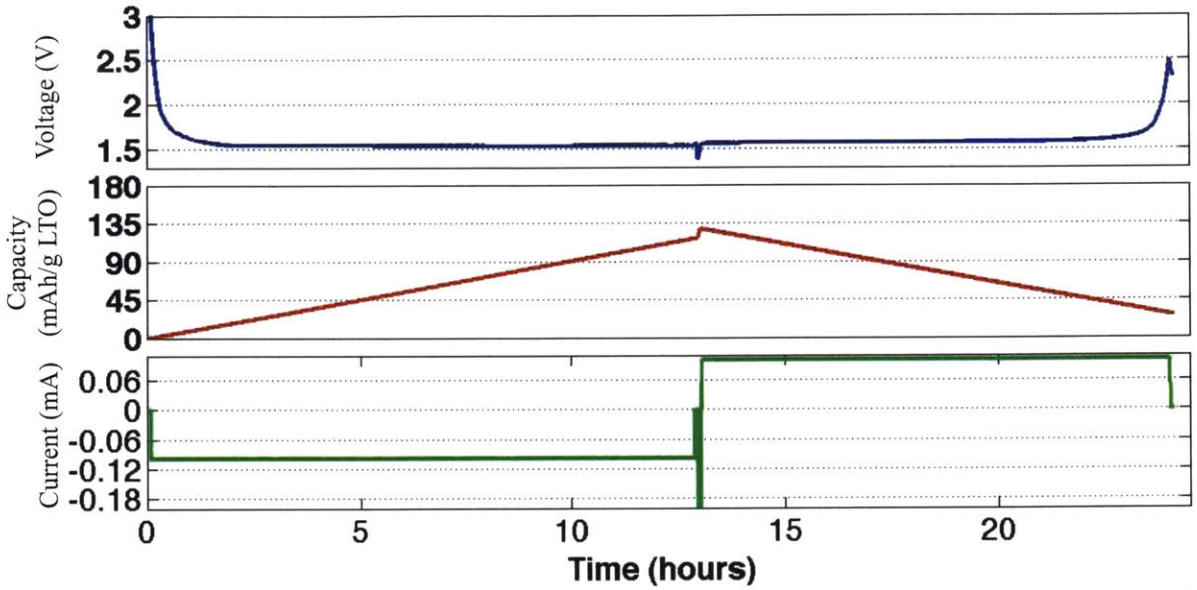

Figure 5.3.2 Voltage, theoretical percent charge and current vs. time profiles for an anode suspension tested in a half static cell setup (experiment Static-Anode-2). The data shows the ability of an suspension of Altairnano LTO and carbon additive to cycle in DMC electrolyte at C/18 rates (specific current = 9.2 mA g^{-1} LTO, current density = 3.1 A m^{-2} Celgard). The high voltage cutoff for galvanostatic charging (1.4 V) was intended to prevent detrimental SEI formation and decreased the reversible capacity of LTO.

maximum theoretical capacity, but this is expected because of the high voltage cutoff (1.4 V). In this testing setup, the voltage of the suspension was not allowed to go below 1.4 V, to prevent decomposition of the DMC electrolyte. The high voltage cutoff limited the polarization that could be applied to the suspension and reduced the available capacity at C/18 rate. The current profile shows a small peak upon charge due to a different charge step at a higher rate, which was cut short to prevent solvent decomposition.

The ability of lithium titanate to charge and discharge in DMC electrolyte while remaining a stable suspension is a highly significant result. Because DMC (dimethyl carbonate mixed with $LiPF_6$) is an organic carbonate electrolyte, it is stable at higher voltages up to 4.5 V vs. Li, at which lithium cobalt oxide cycles. Therefore DMC electrolyte can be used as the single electrolyte in a full cell employing lithium cobalt oxide as the cathode and lithium titanate as the anode in their respective suspensions. Discovering an electrolyte which allows cycling of stable anode and cathode suspension is a crucial step forward towards a full cell with flowing suspensions on both sides.

Table 5.3.2 Description of experimental setup Static-Anode-2.

Test type: half static cell		Current collector: Aluminum		Separator film: Celgard	
Suspension composition:		Coating: Au sputtered (120 s @ 40 mA)		Test cell characteristics:	
Volumetric	By mass:	Suspension characteristics		Well depth	0.5 mm
20.0 % LTO	38.2 % LTO	Theoretical energy density:		Cell volume	15.8 µL
1.0 % Ketjen	1.3 % Ketjen	Volumetric	117.6 Ah/L	Theoretical capacity	1.85 mAh
79.0 % DMC	60.5 % DMC	Gravimetric	65.4 Ah/kg	C rate @ 100 µA	C/18

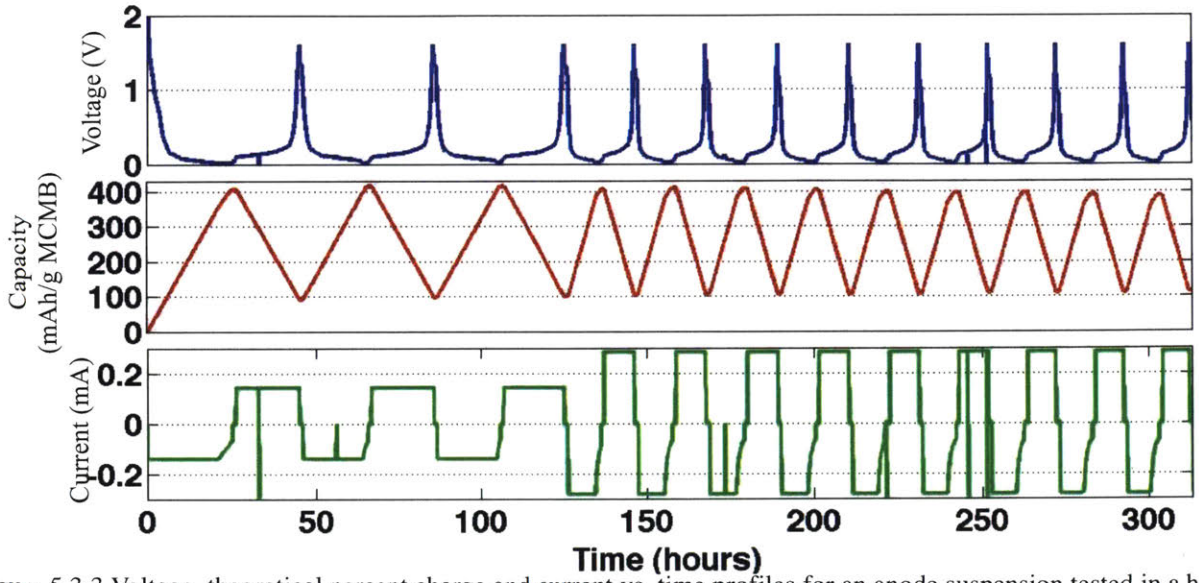

Figure 5.3.3 Voltage, theoretical percent charge and current vs. time profiles for an anode suspension tested in a half static cell setup (experiment Static-Anode-3). The data shows the ability of an suspension of copper-coated graphite (Cu-MCMB 2% copper by mass) in SSDE electrolyte to cycle at C/10 rates (specific current = 36.2 mA g^{-1} Cu-MCMB, current density = 9.0 A m^{-2} Celgard). Data courtesy of Bryan Ho.

Table 5.3.3 Description of experimental setup Static-Anode-3.

Test type: half static cell		Current collector: Copper		Separator film: Celgard	
		Coating: N/A		Test cell characteristics:	
Suspension composition:		Suspension characteristics		Well depth	0.28 mm
Volumetric	By mass:	Theoretical energy density:		Cell volume	8.9 µL
40.4% Cu-MCMB	52.2 % Cu-MCMB	Volumetric	302.2 Ah/L	Theoretical capacity	2.86 mAh
59.6 % SSDE	47.8 % SSDE	Gravimetric	177.8 Ah/kg	C rate @ 286 µA	C/10

As the driving force for SEI formation is higher at potentials close to that of the Li/Li^+ electrode, graphite (lithiation potential = 0.1 V vs. Li/Li^+) was assumed to be more affected by SEI formation than lithium titanate. Figure 5.3.3 represents the voltage, capacity and current vs. time results of a test of copper coated graphite (Cu-MCMB: Meso Carbon Micro Beads) in SSDE electrolyte (organic carbonate mixture with $LiPF_6$ salt) (experiment Static-Anode-3). The content of copper in the MCMB was 2% by mass. Using copper coated graphite (MCMB) was found to decrease the amount of solid electrolyte interface (SEI) compared to as received graphite. The experiment revealed significant irreversible lithium consumption, consistent with SEI formation and typical for the anode material behavior in regular Li-ion batteries. However, analysis of the suspension after the charge / discharge test revealed that the material had transformed from a viscous suspension to a hard, almost dry cake.

5.4 Continuous flow cycling of cathode and anode suspensions

The ability of stable suspensions to store and transport Li^+ ions while under non-zero flow represents a major stepping stone in the development of the SSFC system. The initial tests were performed in half

flow testing cells (see description in section 3.5.3) to evaluate behavior of the suspensions against the reference Li/Li^+ electrode. The two most important constraints in designing and operating a flow cell were the relatively high viscosity of the suspensions and the small diameter of the testing channel needed to reduce electronic and ionic polarizations. The pumping method chosen was peristaltic pumping through a closed loop, of which ~20% was the current collector area. The working assumptions were that peristaltic pumping prevented settling of the particles by constantly providing energy to the suspension. With carefully chosen construction materials, half flow cells allowed repeatable charge / discharge experiments on both anode and cathode slurries.

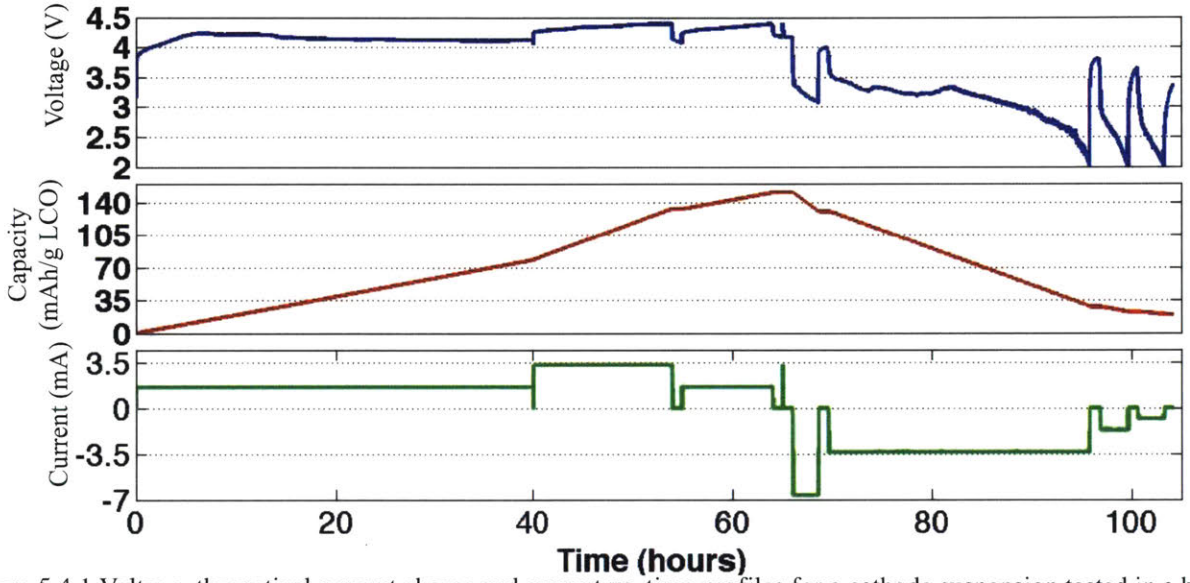

Figure 5.4.1 Voltage, theoretical percent charge and current vs. time profiles for a cathode suspension tested in a half continuous flow cell setup (experiment Continuous-Flow-Cathode-1). At C/7 rate, for the material in the channel: specific current = 18.3 mA g^{-1} LCO, current density = 25.8 A m^{-2} Tonen. The suspension was flowed continuously at 20.3 mL/min for the entire duration of the experiment.

Figure 5.4.1 represents a key achievement in the development of the solid suspension flow cell system. The data represents the first successful charge / discharge experiment of a cathode material (lithium cobalt oxide) suspended in SSDE electrolyte and carbon additive while being flowed through the test cell at a constant rate (experiment Continuous-Flow-Cathode-1). The suspension was flowing at 20.3 mL/min through the loop constantly during the entire experiment. The top curve represents the response of the cell potential to the various currents ran by the cell during charge and discharge. The voltage profile shows clear plateaus during both charge and discharge, confirming that the electrochemical reaction is occurring reversibly. The middle curve, the capacity profile, shows the cell charging to slightly more than the reversible capacity of lithium cobalt oxide (140 mAh/g LCO). The most likely cause of this apparent overcharging is due to the flexibility of the tubing used in the experiment. As the suspension was loaded under significantly high pressure, the tubing could have been overloaded and forced to expand slightly, which would account for the extra capacity of the material. The current profile shows the rates ran across the cell; the highest charge rate was C/33, while

the highest discharge rate was D/16.5. Considering that the current collector area was ~20% of the total length of the loop, the cell was running, at its best, for the material in the channel, approximately instant C/7 and D/3.5 rates. The ability of a suspension to run such high rates, while being under constant flow is a remarkable discovery, and it represents a pivotal achievement for the SSFC system.

Table 5.4.1 Description of experimental setup Continuous-Flow-Cathode-1.

Test type: half flow cell		Current collector: Aluminum		Cell characteristics:	
		Coating: N/A		Channel volume	0.16 mL
Suspension composition:		Separator film: Tonen (area = 1.28 cm^2)		Total volume	0.76 mL
Volumetric	By mass:	Suspension characteristics		Channel capacity	25.1 mAh
22.4 % LCO	51.3 % LCO	Theoretical energy density:		Total capacity	119.4 mAh
0.7 % Ketjen	0.7 % Ketjen	Volumetric:	157.1 Ah/L	Channel C rate @ 3.3 mA	C/7
76.9 % SSDE	48.0 % SSDE	Gravimetric:	71.8 Ah/kg	Total C rate @ 3.3 mA	C/33

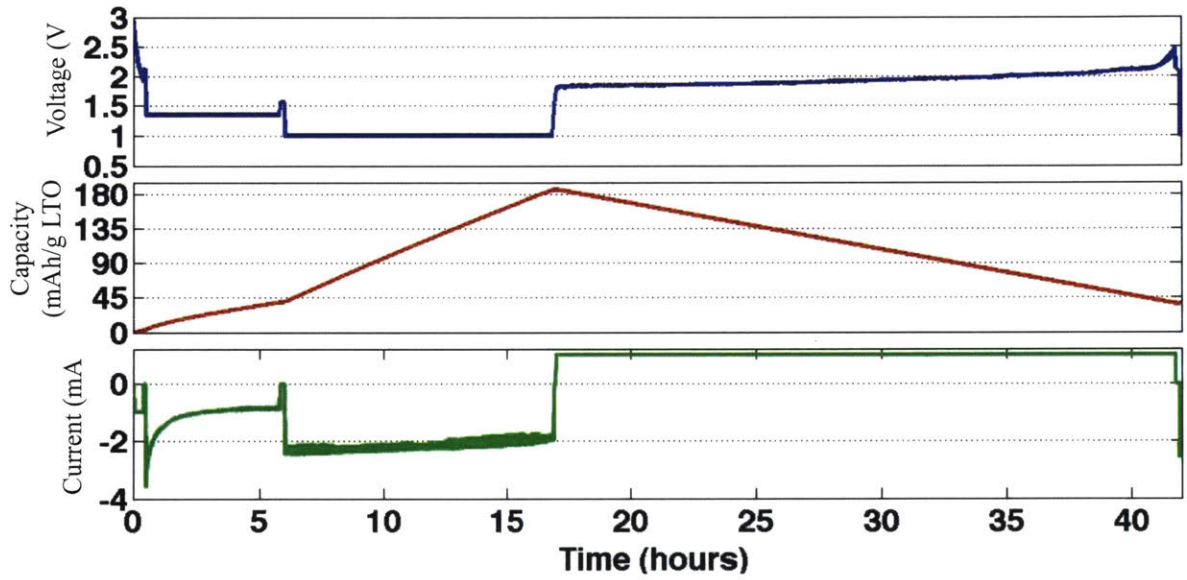

Figure 5.4.2 Voltage, theoretical percent charge and current vs. time profiles for an anode suspension tested in a half continuous flow cell setup (experiment Continuous-Flow-Anode-1). The cell was charged potentiostatically at 1.35 V and at 1.0 V, before being discharged galvanostatically at 17.1 A m^{-2} Tonen. The suspension was continuously flowing through 1/16" diameter tubing at 10 mL/min. The data indicates that the suspension can cycle, but the polarization of the material is high, in spite of the high Ketjen content (LTO to Ketjen ratio is 7.7:1 by mass).

Figure 5.4.2 represents the first successful charge / discharge experiment of an anode material (lithium titanate) suspended in DOL electrolyte and carbon additive while being flowed through the test cell at a constant rate (experiment Continuous-Flow-Anode-1). The voltage profile shows a novel charging method – potentiostatic, by holding the cell at 1.35 and 1.0 V vs. the Li electrode. The purpose of holding the cell at a fixed voltage was to test the stability of the suspension during a charge / discharge experiment, while under constant flow. The results were encouraging as the suspension managed to charge potentistatically, then discharge galvanostatically and still flow out of the test cell at the end of the experiment. One issue which may affect energy density was the high polarization during

discharge, 0.3 – 0.5 V; however, the instantaneous rate in the channel was D/3, considerably high for a material with relatively low electronic conductivity, such as lithium titanate. The result represents a key achievement towards obtaining a full cell in which both the anode and cathode are suspensions of Li-ion battery materials in electrolyte.

The ability of suspensions to charge and discharge under zero flow can be explained by continuous percolation through the carbon additive network which increases the electronic conductivity. However, pumping rates of 20 mL/min imply that a 0.2 mL test channel was replenished more than once a second. Under such conditions, continuous percolation was, most likely, disrupted and the charge and discharge capability must be explained by other phenomena, such as transient percolation or collisions between the active material and carbon additive particles and the current collectors.

Table 5.4.2 Description of experimental setup 4B.

Test type: half flow cell		Current collector: Aluminum		Cell characteristics:	
		Coating: Au sputtered (300 s @ 40 mA)		Channel volume	89.9 μL
Suspension composition:		Separator film: Tonen (area = 0.58 cm^2)		Total volume	0.79 mL
Volumetric	By mass:	Suspension characteristics		Channel capacity	3.1 mAh
5.8 % LTO	13.1 % LTO	Theoretical energy density:		Total capacity	27.9 mAh
1.2 % Ketjen	1.7 % Ketjen	Volumetric:	35.3 Ah/L	Channel D rate @ 1 mA	D/3
93.0 % DOL	85.1 % DOL	Gravimetric:	23.6 Ah/kg	Total D rate @ 1 mA	D/28

The test setup raised a significant concern related to the energy needed for continuous pumping during both charge and discharge. For most suspensions, the pumping energy needed was estimated to be 10-20% of the total discharge energy, depending on the composition and energy density. Such a high energy cost suggested a different test setup: static charge (or discharge) followed by pumping to replenish the material in the test channel.

5.5 Intermittent flow tests of cathode suspensions

The design of the continuous flow experiment placed significant limitations on the composition of the tested suspensions. For cathode mixtures in SSDE (organic carbonate electrolyte) was limited to around 25% LCO, while for anode mixtures in DOL (dioxolane-based electrolyte) it was 15% LTO. Higher loading suspensions would cause mechanical failure of the experimental setup, most often through clogging of the tubing. One way to avoid this problem was to design an intermittent flow experiment, in which the suspensions are pumped in and out only at the beginning and end of the charge/discharge steps.

The setup of an intermittent flow test was similar to a constant flow test in which the peristaltic pump and tubing system had been replaced by glass syringes. Pictures of the experimental setup for intermittent flow tests for half cells and full cells are presented in figures 5.5.1(a) and (b). The pumping

of the suspensions was accomplished through manual control which provided reasonable accuracy. An interesting observation was that suspensions which could cycle under high flow rates (such as that in experiment Continous-Flow-Cathode-1) showed much higher polarization at comparable rates under static conditions. Because of this, higher loadings of carbon additives were employed to reduce polarization in the intermittent flow setup.

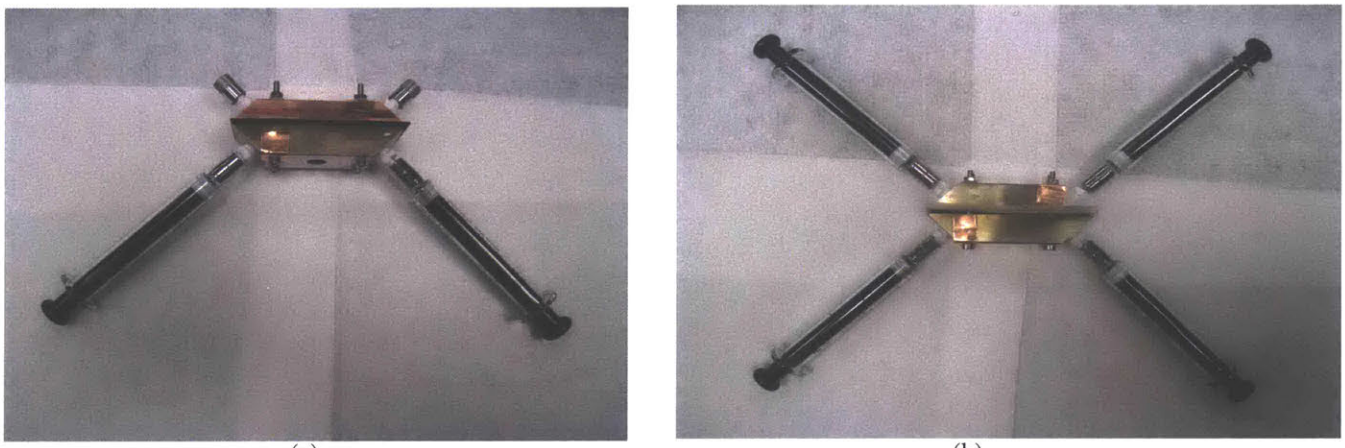

(a) (b)

Figure 5.5.1 (a) Picture of an assembled half flow cell prepared for intermittent flow. The syringes are only used on the active material side to pump the suspension in and out of the cell. (b) Picture of an assembled full flow cell prepared for intermittent flow. The syringes are only used on both sides to pump the suspensions in and out of the cell.

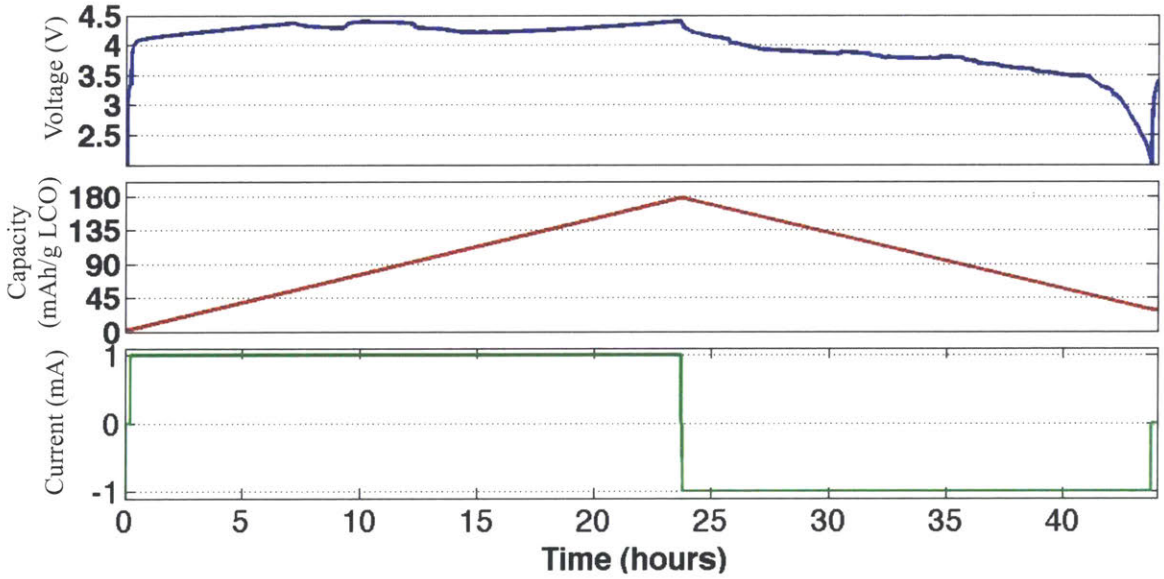

Figure 5.5.2 Voltage, theoretical percent charge and current vs. time profiles for a cathode suspension tested in a half flow cell setup under zero flow (experiment Intermittent-Flow-Cathode-1). At C/19 rate, for the material in the channel: specific current = 7.5 mA g^{-1} LCO, current density = 17.1 A m^{-2} Tonen. The high capacity value for LCO is due to additional charging of the suspension outside the channel, in the inlet and outlet ports.

Figure 5.5.2 shows the voltage and charge vs. time plots for an lithium cobalt oxide suspension cycled once in a flow setup, under zero flow (experiment Intermittent-Flow-Cathode-1). The result is significant in that it proves the feasibility of an intermittent flow setup, in which a single plug of

suspension is charged, stored outside of the cell, and then returned to the cell to be discharged.

Table 5.5.1 Description of experimental setup Intermittent-Flow-Cathode-1.

Test type: half flow cell		Current collector: Aluminum		Cell characteristics:	
Note: suspension held under zero flow		Coating: Au (300 s @ 40 mA)		Channel volume	89.9 µL
Suspension composition:		Separator film: Tonen (area = 0.58 cm^2)		Total volume	89.9 µL
Volumetric	By mass:	Suspension characteristics		Channel capacity	18.8 mAh
30.0 % LCO	60.9 % LCO	Theoretical energy density:		Total capacity	18.8 mAh
0.8 % Ketjen	0.7 % Ketjen	Volumetric:	210.4 Ah/L	Channel C rate @ 1 mA	C/19
69.2 % SSDE	38.4 % SSDE	Gravimetric:	85.3 Ah/kg	Total C rate @ 1 mA	C/19

Considering that the cycle life of suspensions can be proven in static cells, the most significant result consists of the ability to flow after a full charge and discharge experiment. The voltage, capacity and current curves vs. time fit the expected profiles based on previous static cell results. The extra capacity is most likely due to extra charging of the suspension in the inlet and outlet ports, outside the channel. This result suggested that intermittent flow to be a more practical substitute for continuous flow experiments.

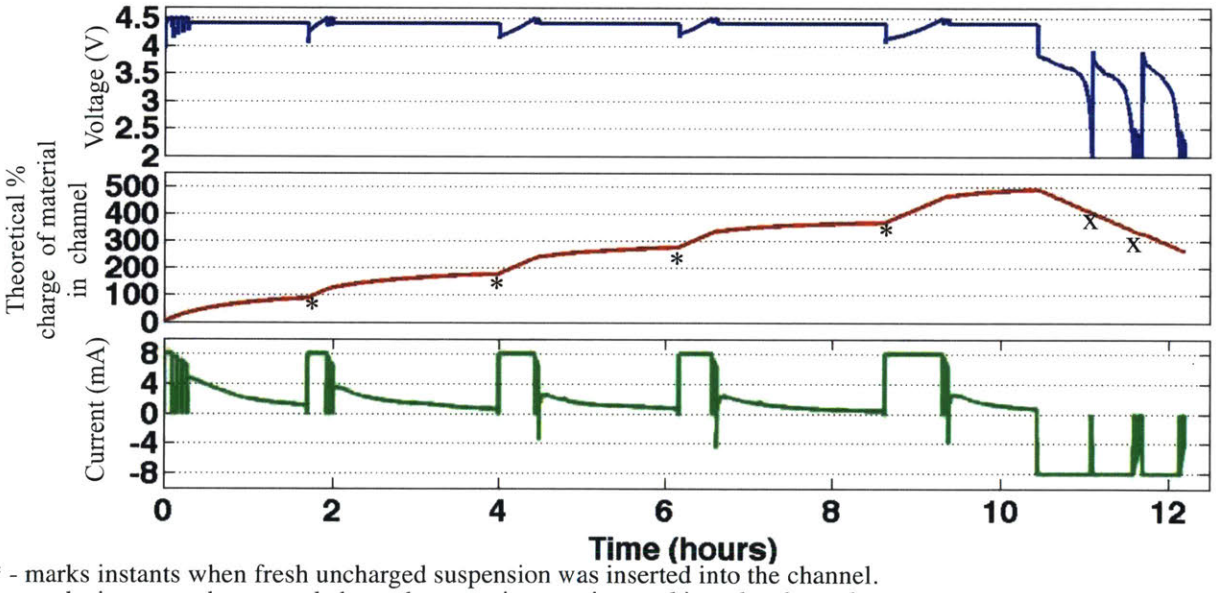

* - marks instants when fresh uncharged suspension was inserted into the channel.
x - marks instants when stored charged suspension was inserted into the channel
Figure 5.5.3 Voltage, theoretical percent charge and current vs. time profiles for a cathode suspension tested in a half flow cell setup under intermittent flow (experiment Intermittent-Flow-Cathode-2). At C/19 rate, for the material in the channel: specific current = 179.4 mA g^{-1} LCO, current density = 136.8 A m^{-2} Tonen. Discharge power density = 478.8 W m^{-2} Tonen, assuming 3.5 V discharge potential.

Experiment Intermittent-Flow-Experiment-1 showed that a suspension containing sufficient carbon additive could be charged and discharged in a flow cell setup. The next step was to charge discrete volumes of suspension, store the charged material outside the cell, then return the suspension into the cell to be discharged. The energy needed for pumping a certain volume of suspension under

these conditions was calculated to be less than 0.4% of the energy stored in that volume.

Table 5.5.2. Description of experimental setup Intermittent-Flow-Cathode-2.

Test type: half flow cell		Current collector: Aluminum		Cell characteristics:	
Note: intermittent flow		Coating: Au (300 s @ 40 mA)		Channel volume	89.9 µL
Suspension composition:		Separator film: Tonen (area = 0.58 cm^2)		Total charged volume	5 x 89.9 µL
Volumetric	By mass:	Suspension characteristics		Total discharged volume	3 x 89.9 µL
10.0 % LCO	28.7 % LCO	Theoretical energy density:		Channel capacity	6.2 mAh
1.5 % Ketjen	1.9 % Ketjen	Volumetric:	70.1 Ah/L	Channel C rate @ 8 mA	1.3C
88.5 % SSDE	79.4 % SSDE	Gravimetric:	40.2 Ah/kg	Channel D rate @ 8 mA	1.3D

Figure 5.5.3 shows a successful intermittent flow charge/discharge experiment on an lithium cobalt oxide (LCO) and Ketjen suspension in SSDE electrolyte. The ability to charge multiple volumes of suspension, store the charged material outside the cell, then return it to the test cell to be discharged, represents a key achievement towards developing an intermittent flow full cell. The cell was charged in a constant current, constant voltage protocol, running 1.3C galvanostatically until the cell voltage was 4.5 V, then held potentiostatically at 4.4 V for 2 hours. Beyond the remarkable intermittent flow result, another interesting fact is the relatively high current and power densities on discharge. The energy efficiency per volume of cell is estimated to be 55.6%, considering that 0.9% of energy is used on pumping of the cell.

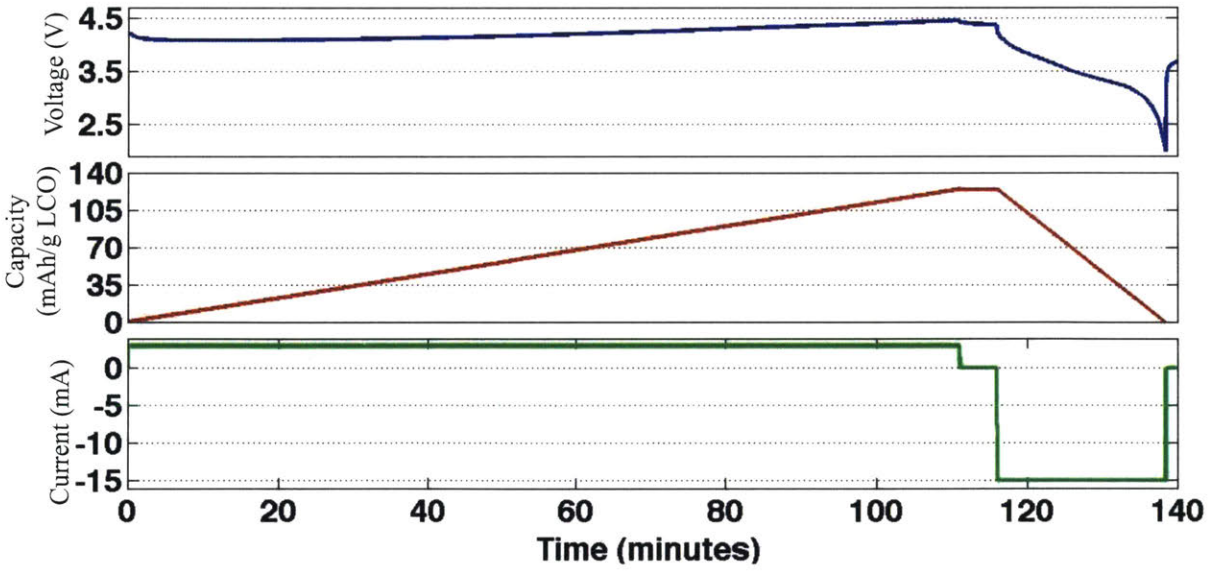

Figure 5.5.4 Voltage, theoretical percent charge and current vs. time profiles for a lithium cobalt oxide cathode suspension tested in a half flow cell setup under zero flow (experiment Intermittent-Flow-Cathode-3). At 2.5D rate, for the material in the channel: specific current = 336.3 mA g^{-1} LCO, current density = 256.8 A m^{-2} Tonen. Discharge power density = 898.8 W m^{-2} Tonen, assuming 3.5 V discharge potential.

Figure 5.5.4 shows another intermittent flow experiment aimed at investigating the power density limit of the suspensions. The test was a single charge / discharge experiment on a lithium cobalt

oxide (LCO) suspension with a high carbon loading in SSDE electrolyte. The charge rate was lower than the discharge rate to prevent dangerous lithium dendrite formation during delithiation (charging) of the cathode suspension. The result is highly significant, as the power density on discharge is relatively high (~1000 W/m^2) which approaches the required range for automotive applications (5000 – 10000 W/m^2). The energy efficiency, 82%, is higher than experiment Intermittent-Flow-Cathode-2 because of several reasons. First, the charge rate is somewhat lower, meaning that the polarization is reduced during delithiation of the material. Second, the test cell was modified to employ thinner spacers (0.017" polypropylene spacers instead of 0.12" - Figure 3.5.5 (a)) and reduced the IR drop across solvent-filled volumes in the cell during both charge and discharge.

The most interesting difference between experiments Intermittent-Flow-Cathode-1 and Intermittent-Flow-Cathode-2 comes from comparing the current densities observed. A mixture with 30% LCO and 0.8% Ketjen by volume is highly polarized at 17.1 $A\,m^{-2}$ while the 10% LCO, 1.5% Ketjen can handle eight times that rate. The difference in rate capability is, most likely, due to the

Table 5.5.3 Description of experimental setup Intermittent-Flow-Cathode-3.

Test type: half flow cell		Current collector: Aluminum		Cell characteristics:	
Note: suspension held under zero flow		Coating: Au (300 s @ 40 mA)		Channel volume	89.9 µL
Suspension composition:		Separator film: Tonen (area = 0.58 cm^2)		Total volume	89.9 µL
Volumetric	By mass:	Suspension characteristics		Channel capacity	6.2 mAh
10.0 % LCO	28.7 % LCO	Theoretical energy density:		Total capacity	6.2 mAh
2.0 % Ketjen	2.5 % Ketjen	Volumetric:	70.1 Ah/L	C rate @ 3.1 mA	C/2
88.0 % SSDE	68.8 % SSDE	Gravimetric:	40.1 Ah/kg	D rate @ -15 mA	2.5 D

differences in cell design between the static and flow setups. First, the static cell has a shorter distance to the nearest segment of current collector, <0.5 mm on average, compared to ~0.8 mm in a flow cell setup. Moreover, the half flow setup has extra volume available on the Li side for mossy lithium to be stored during the charging of the cathode material. This volume is filled only with the electrolyte which causes a significant IR drop directly proportional to the current applied. Meanwhile, not allowing sufficient space for Li deposition during LCO charge can result in formation of Li dendrites which penetrate through the separator film and short the cell. Both of these problems can easily be avoided in a full flow cell in which the anode is another suspension that can uptake Li, and there are no gaps between the anode and cathode sides.

The most significant advantage intermittent flow cells have over continuous flow cells is the energy necessary for pumping the suspension. Table 5.5.4 presents comparative energy estimates for intermittent vs. continuous flow experiments on a 22.4% LCO, 0.7% Ketjen in SSDE suspension. The energy needed for pumping was estimated assuming the work needed to move the suspension was equal to the product of the pressure applied and the volume displaced (20 N for a channel volume). The energy stored in the system was estimated assuming full LCO charge and discharge at 3.5 V. The flow

test was assumed to take 80 hours at 10 mL/min flow rate through 20 cm of tubing and channel. The calculation shows a clear advantage for the intermittent flow setup. Theoretically, using more concentrated suspensions with higher loadings of LCO would decrease the percentage of energy used for pumping. However, more concentrated suspensions are more viscous and require more energy for pumping, using up more of the stored energy of the suspension.

Table 5.5.4 Comparative energy estimates for continuous vs. intermittent flow.

Experiment type	Continuous flow	Intermittent flow
Volume considered	Tubing + channel = 0.99 mL	Channel = 0.089 mL
Energy to circulate through system once	3.38 mJ (assuming 10 mL/min flow rate)	220 mJ (for filling channel once)
# of refills needed	120000	2
Total flow energy	407 J = 0.11 Wh	0.440 J = $1.2 \cdot 10^{-4}$ Wh
Energy density of suspension	0.49 Wh/L	0.49 Wh/L
Maximum discharge energy	0.49 Wh	0.043 Wh
% energy expended on flowing	22.40%	0.28%

The main factors that reduce the energy efficiency of the cell are: polarization drops, which are common for all types of batteries, and pumping losses, which are common for redox flow cells in which the active material must be pumped continuously to bring material in contact with the current collectors. The solid suspension flow cell model has several advantages which are aimed at increasing energy efficiency. By using carbon additives, conductive networks can be formed which eliminate the need for continuous pumping of the suspensions. Moreover, the percolating networks also reduce the polarization drops across the cell, increasing the overall energy efficiency.

5.6 Testing of static suspensions in full cells

The next step after demonstrating that static suspensions can cycle reliably against Li/Li^+ electrodes was operating a full static cell coupling an anode suspension with a cathode one. The main issue regarding this test was the stability of the electrolyte on the anode side. Since experiments had proven that SSDE electrolyte is stable in the 1.5 to 4.5 V interval, while DOL is stable in the 1.0 to 3.3 V interval a full static cell test was envisioned using the two different electrolytes on the two sides. However, the cathode material of choice was LFP, which undergoes a reversible delithiation reaction upon charging around 3.4 V. For the most successful anode electrolyte, DOL, the degradation was found to be much slower around 3.4 V compared to 3.9 V. Therefore, in the case that the two electrolytes were to mix, an LFP-LTO full cell would be stable for a longer time than a LCO-LTO cell.

Figure 5.6.1(a) shows the voltage vs. capacity of a full cell with Nanophosphate™ (abbreviated LFP) (suspended in SSDE electrolyte) against LTO (suspended in DOL electrolyte) (experiment Full-Static-1). This result is a significant milestone towards a flowing full cell, as it proves the ability of two

suspensions to function as anode and cathode in the proposed SSFC redox battery. The data is presented as a profile of cell voltage as a function of the capacity of the anode. Because of the lower loading limit of lithium titanate in electrolyte, compared to Nanophosphate™ , the cell was capacity limited on the anode side. The voltage plateaus are in the correct range (~1.9 V, the difference in the operating potentials of the two components). There is some irreversible capacity loss during the first cycle, most likely due to the decomposition of the solvents which had crossed over to the opposite electrode. Considering the discharge rate of D/5 for the anode, the polarization is to be expected, as well as the reduced reversible capacity. Overall, the result is highly interesting, as it suggests the possibility of operating a 2-electrolyte full cell under flowing conditions, pending the implementation of a robust separator film to prevent solvent mixing.

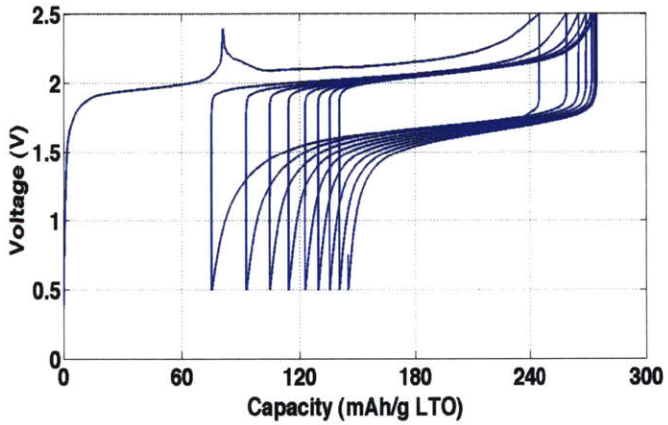

(a)

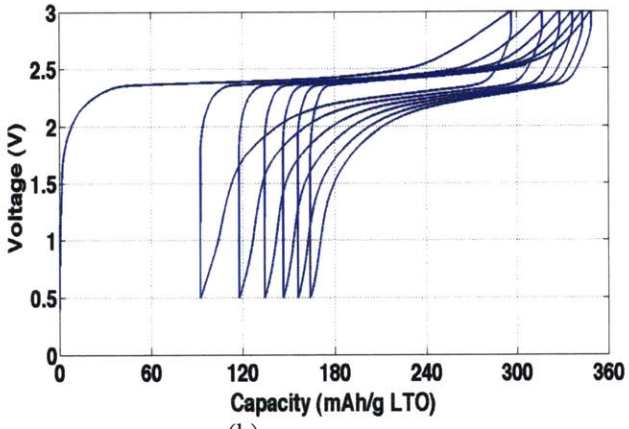

(b)

Figure 5.6.1(a) Voltage vs. specific capacity profile for a cathode suspension tested in a full static cell setup (experiment 6A). The data shows a suspension of Nanophosphate™ (LFP) and carbon additive can cycle against a suspension of LTO and carbon additives in DOL at C/5 (current density = 9.4 A m^{-2} Tonen). (b) Voltage vs. specific capacity profile for a cathode suspension tested in a full static cell setup (experiment 6B). The data shows the ability of a suspension of LCO and carbon additive to cycle against a suspension of LTO and carbon additive in DMC at C/4.5 (current density = 9.4 A m^{-2} Tonen).

Table 5.6.1 Description of experimental setup Full-Static-1.

Type: full static cell		Separator film: Tonen		Side		
Cathode current collector: Al		Coating: Au (300 s @ 40 mA)		Position	Top	Bottom
Anode current collector: Al		Coating: Au (300 s @ 40 mA)		Active material	LFP	LTO
				Electrolyte	SSDE	DOL
				Volumetric capacity	104.0 Ah/L	99.9 Ah/L
Cathode composition		Anode composition		Specific capacity	59.3 Ah/kg	57.7 Ah/kg
Volumetric	By mass:	Volumetric	By mass:	Cell depth	0.63 mm	0.5 mm
17.0 % LFP	34.9 % LFP	17.0 % LTO	34.0 % LTO	Cell volume	20.0 L	15.8 L
0.9 % Ketjen	1.1 % Ketjen	0.9 % Ketjen	1.1 % Ketjen	Cell capacity	2.09 mAh	1.58 mAh
82.1 % SSDE	64.0 % SSDE	82.1 % DOL	64.9 % DOL	C rate @ 300 A	C/7	C/5

The two-electrolyte system had several disadvantages, including low operating voltage (<2 V) and poor stability. Under flowing conditions, the solvents on the two sides were found to mix and

Table 5.6.2 Description of experimental setup Full-Static-2.

Type: full static cell		Separator film: Tonen		Side		
Cathode current collector: Al		Coating: Au (300 s @ 40 mA)		Position	Top	Bottom
Anode current collector: Al		Coating: Au (300 s @ 40 mA)		Active material	LCO	LTO
				Electrolyte	DMC	DMC
				Volumetric capacity	140.1 Ah/L	88.2 Ah/L
Cathode composition		Anode composition		Specific capacity	65.4 Ah/kg	52.3 Ah/kg
Volumetric	By mass:	Volumetric	By mass:	Cell depth	0.3 mm	0.5 mm
20.0 % LCO	48.1 % LCO	15.0 % LTO	30.7 % LTO	Cell volume	10.3 L	15.8 L
1.4 % Ketjen	1.4 % Ketjen	1.0 % Ketjen	1.3 % Ketjen	Cell capacity	1.44 mAh	1.39 mAh
78.6 % DMC	50.5 % DMC	84.0 % DMC	68.0 % DMC	C rate @ 300 A	C/5	C/4.5

undergo decomposition reactions. The solution to these problems was using a single electrolyte which was electrochemically stable in the operating voltage range of the cell. An immediate candidate was DMC (1M LiPF6 in dimethyl carbonate) which allowed LTO to cycle at low polarization. Also, DMC is a carbonate solvent which had been proven to be stable above 4.0 V, at the charge voltages of LCO. The LCO-LTO couple is expected to have a discharge voltage above 2 V and good stability as long as the LTO is kept above 1.3-1.4 V vs. a Li/Li^+ electrode.

Figure 5.6.1(b) shows the voltage vs. capacity of a full cell using lithium cobalt oxide (LCO) as the cathode and lithium titanate (LTO) as the anode, suspended in DMC, (experiment Full-Static-2). This represents a key achievement towards a proof-of-concept full flow cell, as it demonstrates the ability of anode and cathode materials' suspensions in the same electrolyte to function together in transporting and storing Li^+ ions. The data is presented as a profile of cell voltage as a function of the capacity of the anode. Because of the lower loading limit of lithium titanate in electrolyte, compared to lithium cobalt oxide, the cell was capacity limited on the anode side. The voltage plateaus are in the correct range (~2.3 V, the difference in the operating potentials of the two components). There is some irreversible capacity loss during the first cycle, most likely due to partial SEI formation. Considering the discharge rate of D/4.5 for the anode, the polarization across the cell is considered relatively low, while the reversible capacity is promising. This static full cell result represents a major accomplishment towards the construction of a functioning full cell with anode and cathode suspensions operating under intermittent flow.

The voltage vs. capacity curves for both full cells indicate the problem of side reactions: decomposition in the case of DOL and SEI formation for DMC manifests themselves as irreversible capacities. However, the stability of DMC is considered to be high enough to enable full cells with flowing suspensions under intermittent conditions. Considering that DMC only enables the use of lithium titanate as the anode, alternate anode materials require a different approach. Two proposed methods are: implementation of a non-porous separator material (polymer or ceramic) which could keep two solvents separated or discovery and implementation of a solvent which is electrochemically

stable in the 0 to 5 V interval.

5.7 Demonstration of a full cell cycling under intermittent flow

The main goal of this work was to prove the ability of suspensions to serve as anode and cathode for a full operational cell, while under intermittent flow. The key steps towards this goal were: showing that suspensions can cycle in a static environment (Fig. 5.2.1 and 5.3.1), proving that charged material can be stored outside of the cell, then be reinserted for discharge in an intermittent flow setup (Fig. 5.5.3) and demonstrating charge / discharge ability in a full static cell (Fig. 5.6.1). The target experiment (charge/discharge of a full cell) required a robust experimental device which allowed for a reference electrode to be used to measure the potential of the anode independently. The purpose of monitoring the anode potential was to keep the suspension within the safe electrochemical window in which the electrolyte does not decompose (above 1.3 V vs. Li).

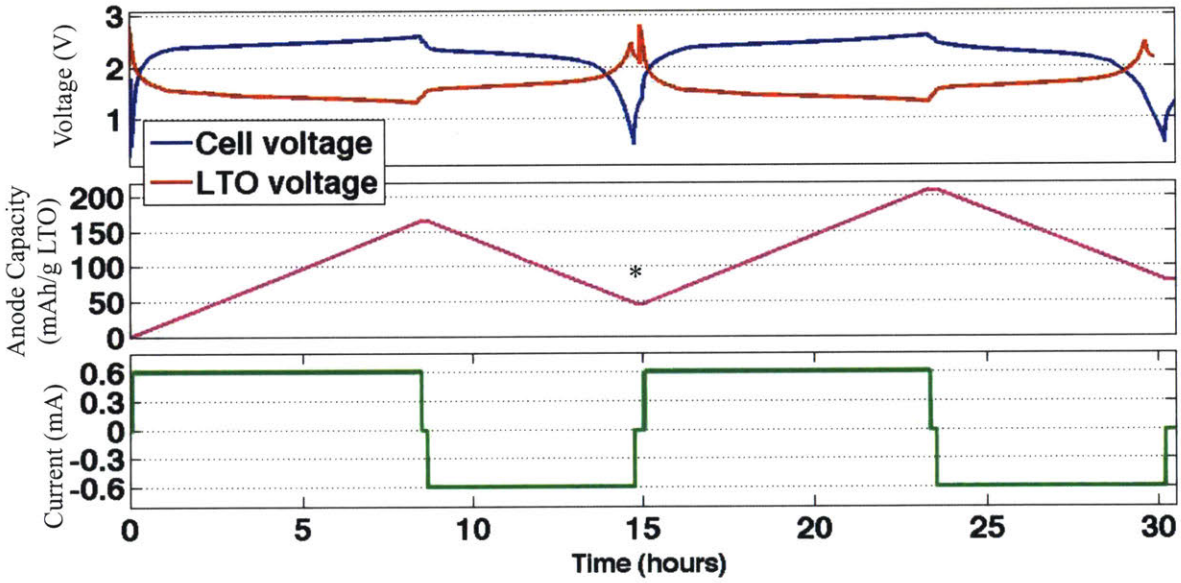

* - marks instants when fresh uncharged suspension was inserted into the channel.
Figure 5.8.1 Voltage, theoretical percent charge and current vs. time profiles for a full flow cell setup under intermittent flow (experiment Intermittent-Flow-Full-1)Cathode: lithium cobalt oxide (LCO), anode: lithium titanate (LTO) suspended in dimethyl carbonate electrolyte (DMC). The voltage profile shows the operating potential of the full cell (blue), as well as the operating potential of the anode (red – measured with a reference electrode). The cell was refilled with At C/8 rate, for the anode material in the channel: current density = 10.3 A m^{-2} Tonen.

Figure 5.8.1 shows two complete charge / discharge cycles for a full cell operating under intermittent flow conditions (experiment Intermittent-Flow-Full-1). The cathode was lithium cobalt oxide and the anode was lithium titanate, both of which were suspended in a mixture of carbon additive and DMC electrolyte. Because of the lower loading limit of the lithium titanate in suspension, as well as the narrower low-voltage stability range of DMC, the anode was capacity limiting. After one

Table 5.8.1 Description of experimental setup Intermittent-Flow-Full-1.

Type: full intermittent flow cell		Separator film: Tonen		Side		
Cathode current collector: Al		Coating: Au (300 s @ 40 mA)		Position	Top	Bottom
Anode current collector: Al		Coating: Au (300 s @ 40 mA)		Active material	LCO	LTO
				Electrolyte	DMC	DMC
				Volumetric capacity	140.1 Ah/L	58.8 Ah/L
Cathode composition		Anode composition		Specific capacity	65.4 Ah/kg	52.3 Ah/kg
Volumetric	By mass:	Volumetric	By mass:	Channel volume	0.09 mL	0.09 mL
20.0 % LCO	48.0 % LCO	10.0 % LTO	21.0 % LTO	Cell capacity	12.5 mAh	5.23 mAh
1.5 % Ketjen	1.5 % Ketjen	2.0 % Ketjen	2.7 % Ketjen	C rate @ 300 A	C/20	C/8
78.6 % DMC	50.5 % DMC	88.0 % DMC	74.3 % DMC			

complete cycle, the test cell was refilled with fresh, uncharged material on both the anode and cathode sides. The top curve, the voltage profile, shows the operating cell voltage (in blue) and the voltage of the anode suspension (in red). The cell voltage is situated in the correct range, around 2.3 V, while the anode voltage plateaus around 1.5 V, as expected. The spike in the anode voltage after the first cycle is due to insertion of fresh, uncharged lithium titanate material. The capacity profile (middle graph) shows some irreversible capacity loss, which may be due to partial SEI formation on the anode side. The current profile (lower graph) shows two consecutive galvanostatic charge / discharge experiments. This represents the single most significant achievement of this entire project, proving that a full cell can operate under intermittent flow. Combined with the previous results (static suspension cycling, full static cell cycling, and intermittent flow cycling of a half cell) this set of data realizes the proof-of-concept of the proposed solid suspension flow cell system.

5.8 Investigation of ethers as possible electrolyte components

The stability of common solvents found in commercial Li-ion batteries is directly dependent on the most polar chemical group found in the molecule. The most stable molecules are, going from 5 to 0 V vs. a Li/Li^+ electrode: carbonates (such as dimethly carbonate), esters (such as γ-butyrolactone) and ethers (such as 1,2-dimethoxyethane, tetrahydrofurane or 1,3-dioxolane).[20] Considering this data, ethers have been implemented as solvents in electrolytes for testing graphite in the solid suspension flow cell system.

Figure 5.8.1 shows voltage vs. capacity data for a suspension of graphite in 2M $LiClO_4$ in 1,3-dioxolane (abbreviated as DXL) (experiment Static-Anode-4). The result is promising from the perspective of enabling a 2-electrolyte full cell, in which the anode would be graphite suspended in DXL electrolyte. The voltage plateaus on charge and discharge are in the right range, around 0.1 V. There is some irreversible capacity exhibited during the first charge step, as some undesired side reactions are occurring.

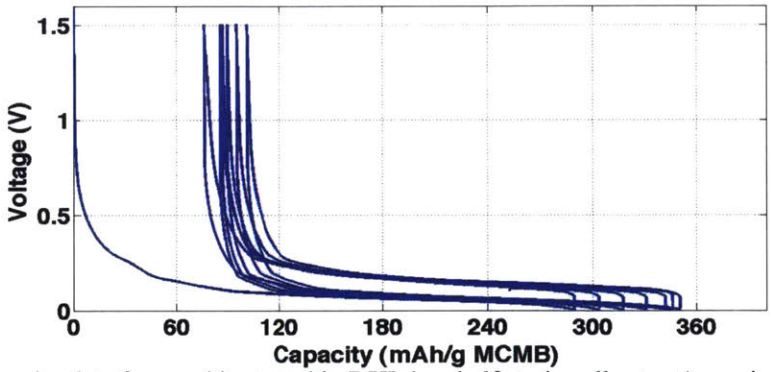

Figure 5.8.1 Voltage vs. capacity data for graphite tested in DXL in a half static cell setup (experiment Static-Anode-4). The data shows the ability of an suspension of MCMB to cycle at C/8 rates with moderate irreversible capacity (specific current = 43.1 mA g^{-1} MCMB, current density = 18.7 A m^{-2} Tonen).

Table 5.8.1 Description of experimental setup Static-Anode-4.

Test type: half static cell		Current collector: Copper		Separator film: Tonen	
Suspension composition:		Coating: N/A		Test cell characteristics:	
		Suspension characteristics		Well depth	0.5 mm
Volumetric	By mass:	Theoretical energy density:		Cell volume	15.8 µL
40.0 % MCMB	51.8 % MCMB	Volumetric	299.2 Ah/L	Theoretical capacity	4.71 mAh
60.0 % DXL	48.2 % DXL	Gravimetric	176.0 Ah/kg	C rate @ 600 µA	C/8

The ability of MCMB to cycle against a Li/Li^+ electrode depends not only on the structures of the solvent and the salt, but also on the salt concentration. Higher salt concentrations, which are desired to improve ion mobility, can also help stabilize the ether solvent molecules by coordinating them to the Li^+ ions.[21] Coordinated solvent molecules are less likely to undergo undesired anodic oxidation reactions which are particularly likely when charging graphite at voltages close to the potential of Li/Li^+. Figure 5.8.2 shows a comparison of 1M and 2M $LiClO_4$ in 1,3-dioxolane used as electrolyte for one charge/discharge cycle of graphite.

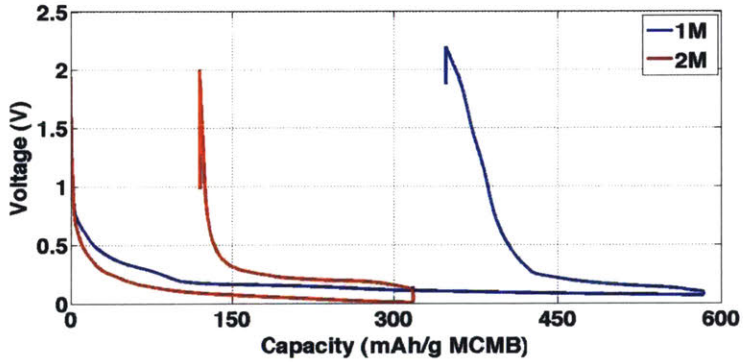

Figure 5.8.2 Comparison of voltage vs. capacity data for graphite tested with 1M and 2M $LiClO_4$ in 1,3-dioxolane in half static cell setups (identical to experimental setup Static-Anode-4). The data shows that for suspensions with the same MCMB loading in identical cells, the suspension containing less Li salt suffers 3x more irreversible capacity loss, while the reversible capacity is relatively similar.

In linear ethers with 4 or more oxygen atoms, the solvent can wrap around the Li^+ ion to form a more stable coordinated cation. At 1:1 molar ratios of solvent to salt, the product of mixing is an ionic liquid of the formula [Li(ether)](anion). Such ionic liquids have been proven to be electrochemically stable in the 0 to 5 V potential range vs. the Li/Li^+ electrode, which makes them excellent candidates for implementation 4 V solid suspension flow cells.

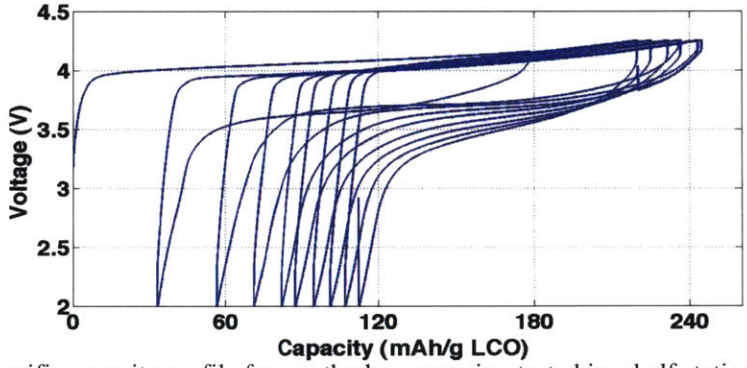

Figure 5.8.3 Voltage vs. specific capacity profile for a cathode suspension tested in a half static cell setup (experiment Static-Cathode-4). The data shows a suspension of LCO and carbon additive in [Li(G4)]TFSI can cycle Li^+ ions against a Li/Li^+ electrode at C/20 rates (specific current = 12.6 mA g^{-1} LCO, current density = 3.2 A m^{-2} Celgard).

Figure 5.8.3 shows the voltage vs. capacity curve for lithium cobalt oxide (LCO) tested in a half static cell in an electrolyte composed of tetraglyme and lithium bis(trifluoromethane)sulfonimide in a 1:1 molar ratio ([Li(G4)]TFSI) (experiment Static-Cathode-4). The result proves that lithium cobalt oxide can cycle in this novel electrolyte maintaining significant reversible capacity (120 mAh/g LCO). The polarization is relatively high for the low rates running across the cell (C/11), which is, most likely, due to the lower ionic conductivity of [Li(G4)]TFSI relative to common organic carbonate electrolytes.

Table 5.8.2 Description of experimental setup Static-Cathode-4.

Test type: half static cell		Current collector: Aluminum		Separator film: Tonen	
Suspension composition:		Coating: Au (300 s @ 40 mA)		Test cell characteristics:	
Volumetric	By mass:	Suspension characteristics		Well depth	0.5 mm
10.0% LCO	28.1% LCO	Theoretical energy density:		Cell volume	15.8 µL
3.0% Ketjen	3.4% Ketjen	Volumetric	70.1 Ah/L	Theoretical capacity	1.10 mAh
87.0% [Li(G4)]TFSI	68.5% [Li(G4)]TFSI	Gravimetric	39.4 Ah/kg	C rate @ 600 µA	C/11

5.9 Future directions

The potential applications of the proposed solid suspension flow cell system depend greatly on the power and energy densities reachable. The energy density is most directly influenced by the amount of active material in the suspension, while the power density depends on both the carbon additive loading, and the operating voltage of the cell. Table 5.9.1 lists the potential ranges in which several cathode and anode materials operate, as well as the stability windows of the electrolytes tested in the SSFC system. Based on the data presented in Table 5.9.1, several electrochemical couples can be envisioned, each with specific properties suitable for a range of applications.

•**Nanophosphate™ – LTO** in **DMC**, operating voltage: **1.9 V**. Main advantages: excellent capacity retention over a large number of cycles for both LTO and LFP, light materials and single electrolyte system. Main disadvantage: SEI formation below 1.3 V for DMC limits how fast the cell can be charged and long term stability.

• **$LiMn_2O_4$ – graphite** in **DXL**, operating voltage: **2.8 V**. Main advantages: relatively higher discharge voltage, high capacity anode and single electrolyte system. Main disadvantage: stability of 1,3-dioxolane above 3.3 V limits the power and capacity of the cell.

• **$Li_2MnO_3 \cdot LiMO_2$ – LTO** in **DMC**, operating voltage: **2.9 V**. Main advantages: relatively higher discharge voltage, excellent capacity retention for the anode material, single electrolyte system. Main disadvantage: DMC stability.

• **$Li_2MnO_3 \cdot LiMO_2$ – 3M anode** or **graphite** in **[Li(G4)]TFSI**, operating voltage: **3.9 – 4.3 V**. Main advantages: high discharge voltage, high capacity materials, single electrolyte system. Main disadvantage: ionic liquid not yet established as reliable electrolyte.

• **$Li_2MnO_3 \cdot LiMO_2$** in **SSDE – 3M anode** or **graphite** in **DXL**, operating voltage: **3.9 – 4.3 V**. Main advantages: established electrolyte compositions, high operating voltage, high capacity materials. Main disadvantage: 2 electrolyte system requires ceramic or polymer separator material to prevent mixing of the solvents.

The wide range of accessible discharge voltages and capacities is an argument for the wide range of potential applications of the SSFC system. For example, the Nanophosphate™ – LTO couple would be a automotive applications high power and energy density are essential, therefore a couple with high operating voltage, such as the $Li_2MnO_3 \cdot LiMO_2$ – 3M anode would be the best fit. Another advantage that the SSFC may have is the ability to use anode materials which are not suited for use in common Li-ion batteries. Anode materials such as Si, Sb and other metals have very

Table 5.9.1 Listing of operating voltages of common Li-ion cathode and anode materials and of stability ranges for potential electrolytes.

Material	Operating voltage (V)	Capacity (mAh/g)	Potential vs. Li (V)	SSDE	DMC	DXL	DOL	[Li(G4)]TFSI
			5					
$Li_2MnO_2 \cdot LiMO_2$*[22]	4.5	250	4.5					
$LiCO_2$	3.9	140	4					
$LiFePO_4$	3.4	170	3.5					
$LiMn_2O_4$ [23]	2.8 – 3.2	140	3					
			2.5					
			2					
LTO	1.55	170	1.5					
Si [24]	0.5 – 1	4200	1					
3M anode [25]	0.4 – 0.5	450	0.5					
Graphite	0.1 – 0.2	340	0					

* - M = Co, Ni, Mn.

high initial capacities (>4000 mAh/g for Si [24]) but suffer from poor cycle life because of the large

volume changes in the lattice structure upon charging (>300% volume change for Si). In the solid electrode setup of common Li-ion batteries, such mechanical stresses are very dangerous for the physical integrity of the cell. However, having the anode suspended in an electrolyte may allow for large volume changes of the particles. Further testing of these materials in the suitable electrolytes will determine the feasibility of this idea.

Table 5.8.2 Comparison of SSFCs with existing flow and fuel cell technologies.

Criteria	Plurion Zn-Ce flow cell [26]	Honda FCX Stack V Flow [27]	Current SSFC results	Target SSFC performance
Operating voltage (V)	2	0.6	2.2 – 3.2	3.2 – 4.0
Current density (A/cm^2)	1000	20000	300	4000
Power density (W/cm^2)	2000	12000	900	12000

The performance of the proposed SSFC is analyzed in relation to current flow and fuel cell technologies; the detailed comparison can be found in table 5.9.2. The current densities achieved in the SSFC system are one order of magnitude less than the current competing technologies. However, the flow cell technology employs fluidized beds to achieve high rates, while fuel cells require current collector foams. Implementation of similar methods is feasible for SSFCs and promises significant current and power density increases. The main advantage SSFCs have is the higher operating voltage, which allows for lower current density targets. Beyond operating voltage, the proposed suspensions also offer conductive, percolating networks which can allow for simpler, less energy intense flow systems. At the moment, the testing devices used for the SSFCs also impose some unnecessary restrictions on current and power densities, which could increase significantly at high operating currents.

Conclusion

The proposed SSFC system was proven to work by cycling anode and cathode suspensions against Li/Li^+ electrodes and against each other. Cathode suspensions were found to work most reliably because of the inherent electrolyte stability at their operating voltages. A series of non-carbonate electrolytes were tested successfully with anode suspensions, revealing the importance of solvent stability.

The suspensions were found to be able to charge and discharge under both flowing and static conditions. The static experimental setup is preferred because of the lower energetic cost of intermittent flow. Full static tests were successfully performed on suspensions of Nanophosphate™ – LTO and LCO – LTO. Cells in which both suspensions were made using the same electrolyte were more reliable and had longer cycle life, but the operating voltage of the cell was limited by the potential stability range of the solvent.

The performance of the SSFC system is highly dependent on suspension composition and testing cell characteristics. The testing devices used limited, in some respects, the cell performance and need to be improved for complete suspension characterization. Several electrochemical couples with stable solvent systems were proposed, as part of a general direction for future development.

Key achievements:

- designing and building robust testing devices for highly tunable static and flow tests;
- demonstration of the first ever lithium cobalt oxide cathode suspension cycling under static conditions in an organic carbonate electrolyte (SSDE);
- demonstration of the first ever lithium titanate suspension cycling under static conditions in a stable dioxolane-based electrolyte (DOL);
- operation of the first ever half flow battery with suspended lithium cobalt oxide working as a cathode under constant flow;
- understanding the importance of electrolyte stability in operating a lithium titanate half flow battery under constant flow;
- demonstration of the first ever single- and two-electrolyte full static cells which employ

suspensions of active material as both the cathode and anode;

- proving the ability of lithium cobalt oxide to store charge outside of a test cell in intermittent flow conditions;
- exploration of alternative ether-based electrolytes to access higher energy density anode materials
- proof-of-concept of the solid suspension flow cell by operating a single electrolyte full cell using lithium cobalt oxide and lithium titanate suspensions under intermittent flow.

The results of this project are a strong support for the development and implementation of solid suspension flow cells as a reliable energy storage system. Beyond proving the feasibility of storing energy in anode and cathode material suspensions, the data shows the SSFC to approach the power density requirements for high power applications, such as fully electric cars. The fundamental concepts behind this system allow for the power and energy densities of these batteries to increase: as novel, high capacity, high voltage materials are discovered, they can easily be suspended in stable electrolytes to be implemented in redox flow cells. Because of the tunability of the suspensions and the ability to decouple the power from the energy stored, this system can offer targeted solutions for a variety of applications ranging from grid level to automotive. As the energy crisis demands innovative solutions, the SSFC system provides new sustainable "fuels" which can be easily stored and transported to serve tomorrow's energy needs.

References:

[1] http://static.howstuffworks.com/gif/lithium-ion-battery-6.jpg Retrieved 3/8/2010.
[2] http://www.netpowertech.com/upFiles/image_yuanli.jpg Retrieved 3/8/2010.
[3] M. Rychcik and M. Skyllas-Kazacos, *J. Power Sources*, 22 (1988) 59-67.
[4] R.J. Remick, P.G.P. Ang, US Patent 4485154 (1984).
[5] Bae et al., *Electrochimica Acta*, 48, (2002), 279-287.
[6] Ponce de Leon et al., *Journal of Power Sources,* 160 (2006), 716-732.
[7] http://upload.wikimedia.org/wikipedia/commons/thumb/9/91/Fluidized_Bed_Reactor_Graphic.svg/ Retrieved 05/03/10.
[8] Evans et al., *Journal of Applied Electrochemistry*, 22 (1992).
[9] Rahman et al., *Journal of Power Sources*, 189 (2009), 1212-1219.
[10] Krause et al., *J. Power Sources* 68 (1997), p. 320.
[11] Parsons, *Solid State Ionics* 94 (1997), 91-98.
[12] Han et al., *Journal of Power Sources*, 92 (2001), 95-101.
[13] Wang et al., *Electrochimica Acta*, 50 (2004), 443-447.
[14] Ge et al., *Electrochemistry Communications*, 10 (2008), 719-722.
[15] Shim et al., *Journal of Power Sources*, 119-121 (2003), 934-937.
[16] Kostecki et al., *Journal of Power Sources*, 136 (2006), 180-184.
[17] Wolfenstine et. al., *Journal of Power Sources*, 154 (2006), 297-289.
[18] Caturla et al., *Journal of the Electrochemical Society*, 142, (1995).
[19] Ross et al., *Journal of the Electrochemical Society*, 148 (2001), A1341-A1345.
[20] Aurbach et al., *Electrochimica Acta* 50 (2004), 247-254.
[21] Watanabe et al., *Journal of Power Sources*, Article in press, 2009.
[22] Thackeray et al., *Electrochemistry Communications* 11(2009).
[23] Bruce et al., *Journal of Power Sources* 54 (1995) 52-57.
[24] Ruffo et al., *J. Phys. Chem. C.* (113 (26), (2009).
[25] Proprietary material composition, operating voltage and capacity data provided by the manufacturer.
[26] Clarke et al., US Patent 7270911 (2009).
[27] Honda Fuel Cell Power, FCX, Press Release 2004.12, http://world.honda.com/FuelCell/FCX/FCXPK.pdf Retrieved 04/21/2010.

Appendix 1. Particle size distribution of materials

Table A1. Particle size distribution for LCO used. Diameters are expressed in microns.

Run #	Sample ID	Classifier RPM	Grinding air PSI	# passes	d(0.1)	d(0.5)	d(0.9)
1	Seimi LCO JM1X	12000	60	1	1.93	4.06	13.19
1a	Seimi LCO JM2X	12000	60	2	1.73	3.44	8.53
2	Seimi LCO JM1X15KCY	15000	60	1	1.65	3.07	7.49
2a	Seimi LCO JM2X15KCY	15000	60	2	1.47	2.47	4.14
3	Seimi LCO JM1XHP15K	15000	80	1	1.58	2.9	7
	Seimi LCO as received				4.66	12.14	28.97

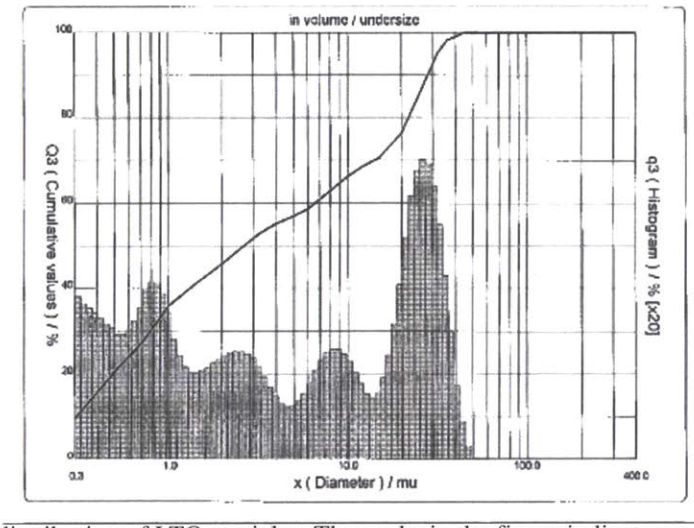

Figure A1.1 Particle size distribution of LTO particles. The peaks in the figure indicate agglomerates. Graph supplied by material manufacturer.

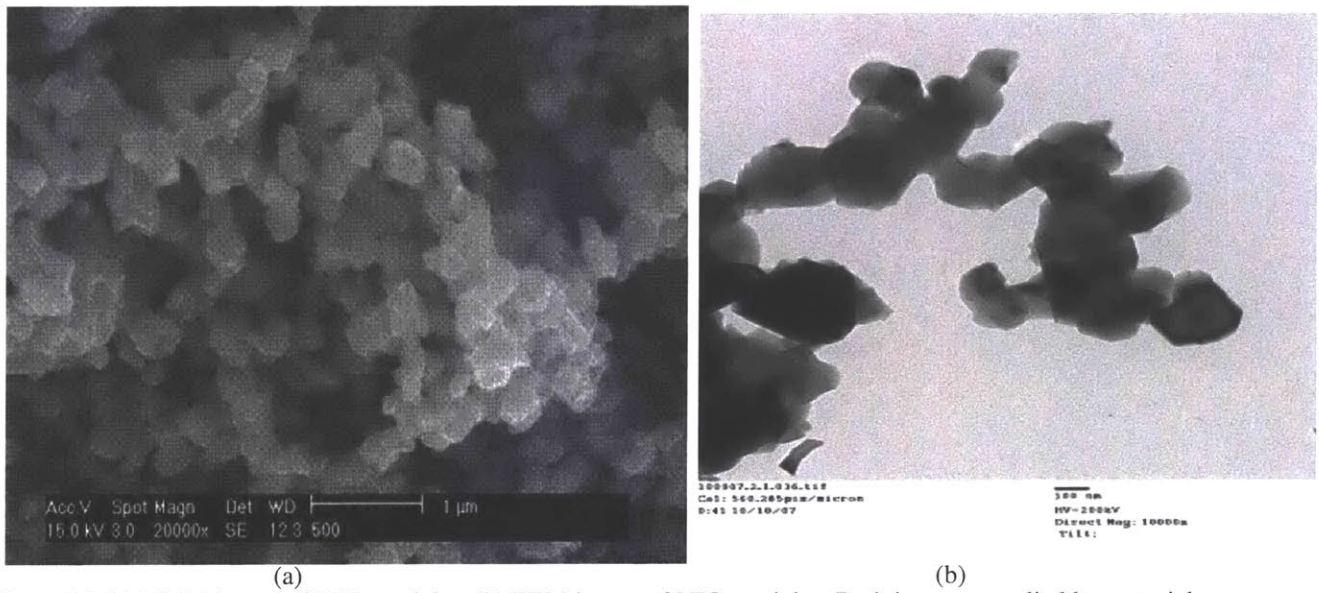

(a) (b)

Figure A1.2(a) SEM image of LTO particles. (b) TEM image of LTO particles. Both images supplied by material manufacturer.